CHAPTER 3

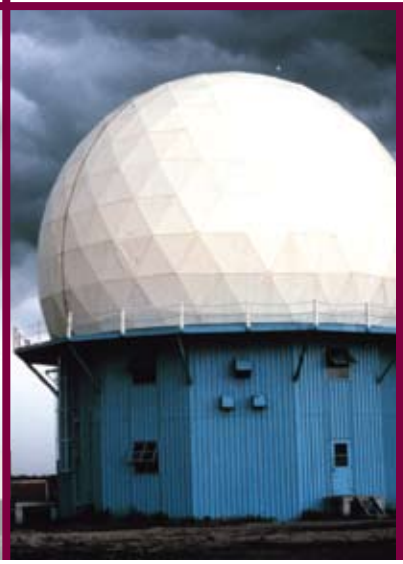

Attribution of the Causes of Climate Variations and Trends over North America during the Modern Reanalysis Period

Convening Lead Author: Martin Hoerling, NOAA/ESRL

Lead Authors: Gabriele Hegerl, Edinburgh Univ.; David Karoly, Univ. of Melbourne; Arun Kumar, NOAA; David Rind, NASA

Contributing Author: Randall Dole, NOAA/ESRL

KEY FINDINGS

- Significant advances have occurred over the past decade in capabilities to attribute causes for observed climate variations and change.
- Methods now exist for establishing attribution for the causes of North American climate variations and trends due to internal climate variations and/or changes in external climate forcing.

Annual, area-averaged change since 1951 across North America shows:

- Seven of the warmest ten years for annual surface temperatures since 1951 have occurred in the last decade (1997 to 2006).
- The 56-year linear trend (1951 to 2006) of annual surface temperature is +0.90°C ±0.1°C (1.6°F ± 0.2°F).
- Virtually all of the warming since 1951 has occurred after 1970.
- More than half of the warming is *likely* the result of anthropogenic greenhouse gas forcing of climate change.
- Changes in ocean temperatures *likely* explain a substantial fraction of the anthropogenic warming of North America.
- There is no discernible trend in average precipitation since 1951, in contrast to trends observed in extreme precipitation events (CCSP, 2008).

Spatial variations in annually-averaged change for the period 1951 to 2006 across North America show:

- Observed surface temperature change has been largest over northern and western North America, with up to +2°C (3.6°F) warming in 56 years over Alaska, the Yukon Territories, Alberta, and Saskatchewan.
- Observed surface temperature change has been smallest over the southern United States and eastern Canada, where no significant trends have occurred.
- There is *very high* confidence that changes in atmospheric wind patterns have occurred, based upon reanalysis data, and that these wind pattern changes are the *likely* physical basis for much of the spatial variations in surface temperature change over North America, especially during winter.
- The spatial variations in surface temperature change over North America are *unlikely* to be the result of anthropogenic forcing alone.
- The spatial variations in surface temperature change over North America are *very likely* influenced by variations in global sea surface temperatures through the effects of the latter on atmospheric circulation, especially during winter.

Spatial variations of seasonal average change for the period 1951 to 2006 across the United States show:

- Six of the warmest 10 summers and winters for the contiguous United States average surface temperatures from 1951 to 2006 have occurred in the last decade (1997 to 2006).
- During summer, surface temperatures have warmed most over western states, with insignificant change between the Rocky Mountains and the Appalachian Mountains. During winter, surface temperatures have warmed most over northern and western states, with insignificant change over the central Gulf of Mexico and Maine.
- The spatial variations in summertime surface temperature change are *unlikely* to be the result of anthropogenic greenhouse forcings alone.
- The spatial variations and seasonal differences in precipitation change are *unlikely* to be the result of anthropogenic greenhouse forcings alone.
- Some of the spatial variations and seasonal differences in precipitation change and variations are *likely* the result of regional variations in sea surface temperatures.

An assessment to identify and attribute the causes of abrupt climate change over North America for the period 1951 to 2006 shows:

- There are limitations for detecting rapid climate shifts and distinguishing these shifts from quasi-cyclical variations because current reanalysis data only extends back to the mid-twentieth century. Reanalysis over a longer time period is needed to distinguish between these possibilities with scientific confidence.

An assessment to determine trends and attribute causes for droughts for the period 1951 to 2006 shows:

- It is *unlikely* that a systematic change has occurred in either the frequency or area coverage of severe drought over the contiguous United States from the mid-twentieth century to the present.
- It is *very likely* that short-term (monthly-to-seasonal) severe droughts that have impacted North America during the past half-century are mostly due to atmospheric variability, in some cases amplified by local soil moisture conditions.
- It is *likely* that sea surface temperature anomalies have been important in forcing long-term (multi-year) severe droughts that have impacted North America during the past half-century.
- It is *likely* that anthropogenic warming has increased drought impacts over North America in recent decades through increased water stresses associated with warmer conditions, but the magnitude of the effect is uncertain.

INTRODUCTION

Increasingly, climate scientists are being asked to go beyond descriptions of *what* the current climate conditions are and how they compare with the past, to also explain *why* climate is evolving as observed; that is, to provide attribution of the causes for observed climate variations and change.

Today, a fundamental concern for policy makers is to understand the extent to which anthropogenic factors and natural climate variations are responsible for the observed evolution of climate. A central focus for such efforts, as articulated in the Intergovernmental Panel on Climate Change (IPCC) Assessment Reports (IPCC, 2007a) has been to establish the cause, or causes, for globally averaged temperature increases over roughly the past century. However, requests for climate attribution far transcend

Today, a fundamental concern for policy makers is to understand the extent to which anthropogenic factors and natural climate variations are responsible for the observed evolution of climate.

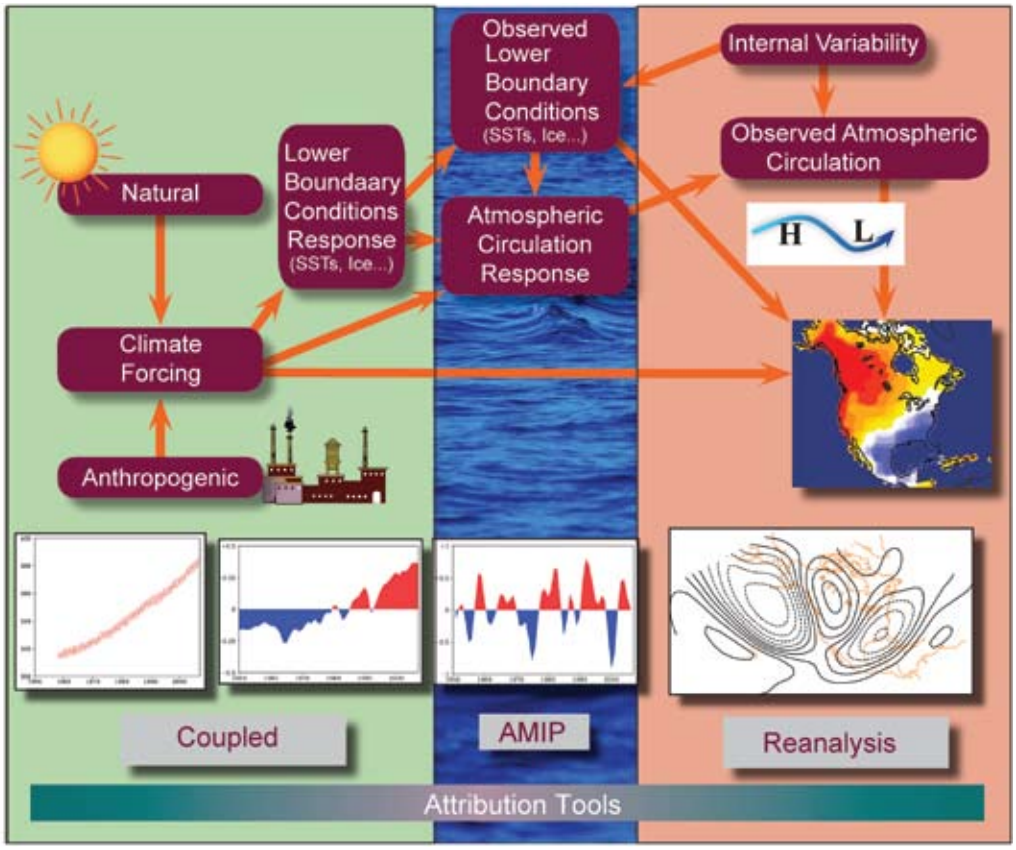

Figure 3.1 Schematic illustration of the datasets and modeling strategies for performing attribution. The map of North America on the right side displays a climate condition whose origin is in question. Various candidate causal mechanisms are illustrated in the right-to-left sequences of figures, together with the attribution tool. Listed above each in maroon boxes is a plausible cause that could be assigned to the demonstrated mechanism depending upon the diagnosis of forcing-response relationships derived from attribution methods. The efficacy of the first mechanism is tested, often empirically, by determining consistency with patterns of atmospheric variability, such as the teleconnection processes (climate anomalies over different geographical regions that are linked by a common cause) identifiable from reanalysis data. This step places the current condition within a global and historical context. The efficacy of the second mechanism tests the role of boundary forcings, most often with atmospheric models (e.g., Atmospheric Model Intercomparison Project, AMIP). The efficacy of the third mechanism tests the role of natural or anthropogenic influences, most often with linked ocean-atmosphere models. The processes responsible for the climate condition in question may, or may not, involve teleconnections, but may result from local changes in direct radiative effect on climate change or other near-surface forcing such as from land surface anomalies. The lower panels illustrate the representative processes: from left-to-right; time-evolving atmospheric carbon dioxide at Mauna Loa, Hawaii, the warming trend over several decades in tropical Indian Ocean/West Pacific warm pool sea surface temperatures (SSTs), the yearly SST variability over the tropical east Pacific due to the El Niño-Southern Oscillation (ENSO), the atmospheric pattern over the North Pacific/North America referred to as the Pacific North American (PNA) teleconnection.

global temperature change alone, with notable interest in explaining regional temperature variations and the causes for high-impact climate events, such as the recent multi-year drought in the western United States and the record setting U.S. warmth in 2006. For many decision makers who must assess potential impacts and management options, a particularly important question is: What are the causes for regional and seasonal differences in climate variations and trends, and how well do we understand them? For example, is the recent drought in the western United States due mainly to factors internal to the climate system (*e.g.*, the sea surface temperature variations associated with ENSO), in which case a return toward previous climate conditions might be anticipated, or is it a manifestation of a longer-term trend toward increasing aridity in the region that is driven primarily by anthropogenic forcing? Why do some droughts last longer than others? Such examples illustrate that, in order to support informed decision making, the capability to attribute causes for past and current climate conditions can be a major consideration.

For many decision makers who must assess potential impacts and management options, a particularly important question is: What are the causes for regional and seasonal differences in climate variations and trends, and how well do we understand them?

The recently completed IPCC Fourth Assessment Report (AR4) from Working Group I contains a full chapter (Chapter 9) devoted to the topic "Understanding and Attributing Climate Change" (IPCC, 2007a). This Chapter attempts to minimize overlap with the IPCC Report by focusing on a subset of questions of particular interest to the U.S. public, decision makers, and policy makers that may not have been covered in detail (or in some cases, at all) in the IPCC Report. The specific emphasis here is on present scientific capabilities to attribute the causes for observed climate variations and change over North America. For a more detailed discussion of attribution, especially for other regions and at the global scale, the interested reader is referred to Chapter 9 of the AR4 Working Group I Report (IPCC, 2007a).

Figure 3.1 illustrates methods and tools used in climate attribution. The North American map (right side) shows an observed surface condition, the causes of which are sought. A roadmap for attribution involves the systematic probing of cause-effect relationships. Plausible factors that contribute to the change are identified along the top of Figure 3.1 (maroon boxes), and arrows illustrate connections among these as well as pathways for explaining the observed condition.

The attribution process begins by examining conditions of atmospheric wind patterns (also called circulation patterns) that coincide with the North American surface climate anomaly. It is possible, for instance, that the surface condition evolved concurrently with a change in the tropospheric jet stream, such as accompanies the Pacific-North American pattern (see Chapter 2). Reanalysis data are essential for this purpose because they provide a global description of the state of the troposphere (the lowest region of the atmosphere which extends from the Earth's surface to around 10 kilometers, or about 6 miles, in altitude) that is physically consistent in space and time. Although reanalysis can illuminate a connection between atmospheric circulation patterns and surface climate, it may not directly implicate the causes, that is, provide attribution.

Additional tools are often needed to explain the atmospheric circulation pattern itself. Is it, for instance, due to chaotic internal atmospheric variations, or is it related to forcing external to the atmosphere (*e.g.*, changes in sea surface temperatures or solar forcing)? The middle column in Figure 3.1 illustrates the common approach used to assess the forcing-response associated with Earth's surface boundary conditions (physical conditions at a given boundary), in particular sea surface temperatures. The principal tool is atmospheric general circulation models that are forced, that is, are subjected to a specific influence (see Box 3.2), for example, a specified history of sea surface temperatures as boundary conditions (Gates, 1992). Reanalysis would continue to be important in this stage of attribution in order to evaluate the suitability of the models as an attribution tool, including the realism of simulated circulation variability (Box 3.1).

In the event that diagnosis of the Atmospheric Model Intercomparison Project (AMIP) simulation fails to confirm a role for Earth's lower boundary conditions, then two plausible explanations for the atmospheric circulation (and its associated North American surface condition) remain. One explanation is that it was due to

chaotic atmospheric variability rather than natural or anthropogenic influences. Reanalysis data would be useful to determine whether the circulation state was within the scope of known variations during the reanalysis record. The other possible explanation is that external natural (*e.g.*, volcanic and solar) or external anthropogenic perturbations may directly have caused the responsible circulation pattern. Coupled ocean-atmosphere climate models would be used to explore the forcing-response relationships involving such external forcings. As illustrated by the left column, coupled models have been widely employed in the Reports of the IPCC. Here again, reanalysis is important for assessing the suitability of this attribution tool, including the realism of simulated ocean-atmosphere variations such as the El Niño-Southern Oscillation (ENSO) and accompanying atmospheric teleconnections (climate anomalies over different geographical regions that are linked by a common cause) that influence North American surface climate (Box 3.1).

If diagnosis of the AMIP simulations confirms a role for Earth's lower boundary conditions, it becomes important to explain the cause for the boundary condition itself. Comparison of the observed sea surface temperatures with coupled model simulations would be the principal approach. If externally-forced models that consider human influences on climate change fail to yield the observed boundary conditions, then the boundary condition may be attributed to chaotic intrinsic coupled ocean-atmosphere variations. If coupled models instead replicate the observed boundary conditions, this establishes a consistency with external forcing as an ultimate cause. (In addition, it is necessary to confirm that the coupled models also generate the atmospheric circulation patterns; that is, to demonstrate that the model result is obtained for the correct physical reason.)

Figure 3.1 illustrates basic approaches applied in the following sections of Chapter 3. It is evident that a physically-based scientific interpretation for the causes of a climate condition requires accurately measured and analyzed features of the time and space characteristics of atmospheric circulation and surface conditions. In addition, the interpretation relies heavily upon the use of climate models to test candidate cause-effect relations. Reanalysis is essential for both components of such attribution science.

While this Chapter considers the approximate period covered by modern reanalyses (roughly 1950 to the present), datasets other than reanalyses, such as gridded surface station analyses of temperature and precipitation, are also used. The surface conditions illustrated in Figure 3.1 are generally derived from such datasets, and these are extensively used to describe various key features of the recent North American climate variability in Chapter 3. These, together with modern reanalysis data, provide a necessary historical context against which the uniqueness of current climate conditions both at Earth's surface and in the free atmosphere can be assessed.

Climate attribution is a scientific process for establishing the principal causes or physical explanation for observed climate conditions and phenomena.

3.1 CLIMATE ATTRIBUTION AND SCIENTIFIC METHODS USED FOR ESTABLISHING ATTRIBUTION

3.1.1 What is Attribution?

Climate attribution is a scientific process for establishing the principal causes or physical explanation for observed climate conditions and phenomena. Within its Reports, the IPCC states that "attribution of causes of *climate change* is the process of establishing the most likely causes for the detected change with some level of confidence" (IPCC 2007). As noted in the Introduction, the definition is expanded in this Product to include attribution of the causes of observed *climate variations* that may not be unusual in a statistical sense but for which great public interest exists because they produce major societal impacts.

It is useful to outline some general classes of mechanisms that may produce climate variations or change. One important class is *external forcing*, which contains both *natural* and *anthropogenic* sources. Examples of natural external forcing include solar variability and volcanic eruptions. Examples of anthropogenic forcing are changing concentrations of greenhouse gases and aerosols and land cover changes produced by human activities. A second class involves *internal mechanisms* within the climate system that can produce climate

BOX 3.1: Assessing Model Suitability

A principal tool for attributing the causes of climate variations and change involves climate models. For instance, atmospheric models using specified sea surface temperatures are widely used to assess the impact of El Niño on seasonal climate variations. Coupled ocean-atmosphere models using specified atmospheric chemical constituents are widely used to assess the impact of greenhouse gases on detected changes in climate conditions. One prerequisite for the use of models as tools is their capacity to simulate the known leading patterns of atmospheric (and for the coupled models, oceanic) modes of variations. Realism of the models enhances confidence in their use for probing forcing-response relationships, and it is for this reason that an entire chapter of the Intergovernmental Panel on Climate Change (IPCC) Fourth Assessment Report (AR4) is devoted to evaluation of the models for simulating known features of large-scale climate variability. That report emphasizes the considerable scrutiny and evaluations under which these models are being placed, making it "less likely that significant model errors are being overlooked". Reanalysis data of global climate variability of the past half-century provide valuable benchmarks against which key features of model simulations can be meaningfully assessed.

The box figure illustrates a simple use of reanalysis for validation of models that are employed for attribution elsewhere in this report. Chapter 8 of the Working Group I report of IPCC AR4 and the references therein provide numerous additional examples of validation studies of the IPCC coupled models that are used in this SAP. Shown are the leading winter patterns of atmospheric variability, discussed previously in Chapter 2 (Figures 2.8 and 2.9), that have strong influence on North American climate. These are the Pacific-North American pattern (left), the North Atlantic Oscillation pattern (middle), and the El Niño-Southern Oscillation pattern (right). The spatial expressions of these patterns is depicted using correlations between observed (simulated) indices of the PNA, NAO, and ENSO with wintertime 500 hectoPascals geopotential heights derived from reanalysis (simulation) data for 1951 to 2006. Both atmospheric (middle) and coupled ocean-atmospheric (bottom) models realistically simulate the phase and spatial scales of the observed (top) patterns over the Pacific-North American domain. The correlations within the PNA and NAO centers of action are close to those observed indicating the fidelity of the models in generating these atmospheric teleconnections. The ENSO correlations are appreciably weaker in the models than in reanalysis. This is in part due to averaging over multiple models and multiple realizations of the same model. It perhaps also indicates that the tropical-extratropical interactions in these models is weaker than observed, and for the CMIP runs it may also indicate weaker ENSO sea surface temperature variability. These circulation patterns are less pronounced during summer, at which time climate variations become more dependant upon local processes (*e.g.*, convection and land-surface interaction) which poses a greater challenge to climate models.

More advanced applications of reanalysis data to evaluate models include budget diagnoses that test the realism of physical processes associated with climate variations, frequency analysis of the time scales of variations, and multivariate analysis to assess the realism of coupling between surface and atmospheric fields. It should be noted that despite the exhaustive evaluations that can be conducted, model assessments are not always conclusive about their suitability as an attribution tool. First, the tolerance to biases in models needed to produce reliable assessment of cause-effect relationships is not well understood. It is partly for this reason that large multi-model ensemble methods are employed for attribution studies in order to reduce the random component of biases that exist across individual models. Second, even when known features of the climate system are judged to be realistically simulated in models, there is no assurance that the modeled response to increased greenhouse gas emissions will likewise be realistic under future scenarios. Therefore attribution studies (IPCC, Chapter 9) compare observed with climate model simulated change because such sensitivity is difficult to evaluate from historical observations.

variations manifesting themselves over seasons, decades, and longer. Internal mechanisms include processes that are due primarily to interactions within the atmosphere as well as those that involve coupling the atmosphere with various components of the climate system. Climate variability due to purely internal mechanisms is often called *internal variability.*

For attribution to be established, the relationship between the observed climate state and the proposed causal mechanism needs to be demonstrated, and alternative explanations need to be determined as unlikely. In the case of attributing the cause of a climate condition to internal variations, for example, due to ENSO-related tropical east Pacific sea surface conditions, the influence of alternative modes of internal climate variability must also be assessed. Before attributing a climate condition to anthropogenic forcing, it is important to determine whether the climate condition was

BOX 3.1: Assessing Model Suitability *Cont'd*

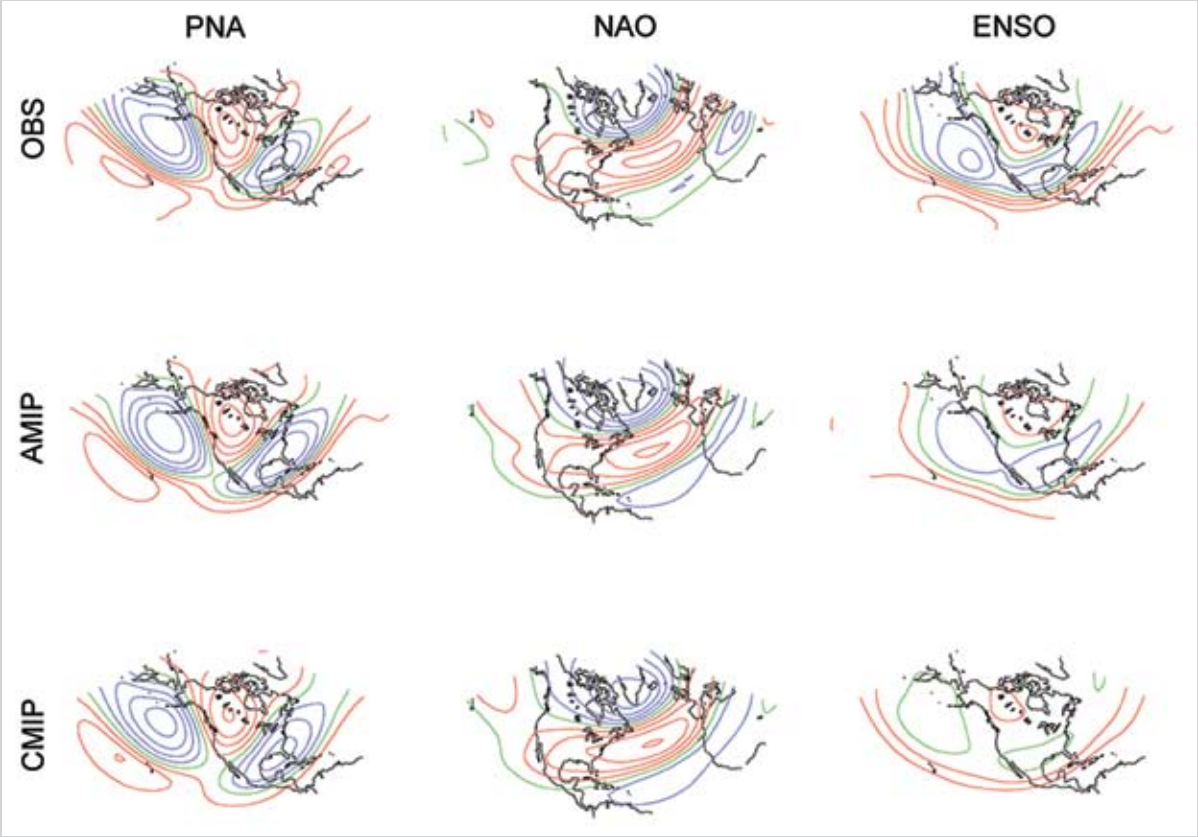

Figure Box 3.1 Temporal correlation between winter season (December, January, February) 500 hectoPascals (hPa) geopotential heights and indices of the leading patterns of Northern Hemisphere climate variability: Pacific-North American (PNA, left), North Atlantic Oscillation (middle), and El Niño-Southern Oscillation (ENSO, right) circulation patterns. The ENSO index is based on equatorial Pacific sea surface temperatures averaged 170°W to 120°W, 5°N to 5°S, and the PNA and NAO indices based on averaging heights within centers of maximum observed height variability following Wallace and Gutzler (1981). Assessment period is 1951 to 2006: observations based on reanalysis data (top), simulations based on atmospheric climate models forced by observed specified sea surface temperature variability (middle), and coupled ocean-atmosphere models forced by observed greenhouse gas, atmospheric aerosols, solar and volcanic variability (bottom). AMIP comprised of 2 models and 33 total simulations. CMIP comprised of 19 models and 41 total simulations. Positive (negative) correlations in red (blue) contours.

unlikely to have resulted from natural external forcing or internal variations alone.

Attribution is associated with the process of explaining the cause of a detected change. In particular, attribution of anthropogenic climate change—the focus of the IPCC Reports (Houghton *et al.*, 1996; IPCC, 2001; IPCC, 2007a)—has the specific objective of explaining a detected climate change that is significantly different from that which could be expected from natural external forcing or internal variations of the climate system. According to the IPCC Third Assessment Report, the attribution requirements for a detected change are: (1) a demonstrated consistency with a combination of anthropogenic and natural external forcings, and (2) an inconsistency with "alternative, physically plausible explanations of recent climate change that exclude important elements of the given combination of forcings" (IPCC, 2001).

3.1.2 How is Attribution Performed?

The methods used for attributing the causes for observed climate conditions depend on the specific problem or context. To establish the cause, it is necessary to identify possible forcings, determine the responses produced by such forcings, and determine the agreement between the forced response and the observed condition. It is also necessary to demonstrate that the observed climate condition is unlikely to have originated from other forcing mechanisms.

Table 3.1 Acronyms of climate models referenced in this Chapter. All 19 models performed simulations of twentieth century climate change ("20CEN") as well as the 720 parts per million (ppm) stabilization scenario (SRESA1B) in support of the IPCC Fourth Assessment Report (IPCC, 2007a). The ensemble size (ES) is the number of independent realizations of the 20CEN experiment that were analyzed here.

	Model Acronym	Country	Institution	ES
1	CCCma-CGCM3.1(T47)	Canada	Canadian Centre for Climate Modelling and Analysis	1
2	CCSM3	United States	National Center for Atmospheric Research	6
3	CNRM-CM3	France	Météo-France/Centre National de Recherches Météorologiques	1
4	CSIRO-Mk3.0	Australia	CSIRO[a] Marine and Atmospheric Research	1
5	ECHAM5/MPI-OM	Germany	Max-Planck Institute for Meteorology	3
6	FGOALS-g1.0	China	Institute for Atmospheric Physics	1
7	GFDL-CM2.0	United States	Geophysical Fluid Dynamics Laboratory	1
8	GFDL-CM2.1	United States	Geophysical Fluid Dynamics Laboratory	1
9	GISS-AOM	United States	Goddard Institute for Space Studies	2
10	GISS-EH	United States	Goddard Institute for Space Studies	3
11	GISS-ER	United States	Goddard Institute for Space Studies	2
12	INM-CM3.0	Russia	Institute for Numerical Mathematics	1
13	IPSL-CM4	France	Institute Pierre Simon Laplace	1
14	MIROC3.2(medres)	Japan	Center for Climate System Research/ NIES[b]/JAMSTEC[c]	3
15	MIROC3.2(hires)	Japan	Center for Climate System Research/ NIES[b]/JAMSTEC[c]	1
16	MRI-CGCM2.3.2	Japan	Meteorological Research Institute	5
17	PCM	United States	National Center for Atmospheric Research	4
18	UKMO-HadCM3	United Kingdom	Hadley Centre for Climate Prediction and Research	1
19	UKMO-HadGEM1	United Kingdom	Hadley Centre for Climate Prediction and Research	1

[a] CSIRO is the Commonwealth Scientific and Industrial Research Organization.

[b] NIES is the National Institute for Environmental Studies.

[c] JAMSTEC is the Frontier Research Center for Global Change in Japan.

The methods for signal identification, as discussed in more detail below, involve both empirical analysis of past climate relationships and experiments with climate models in which forcing-response relations are evaluated. Similarly, estimates of internal variability can be derived from the instrumental records of historical data including reanalyses and from simulations performed by climate models in the absence of the candidate forcings. Both empirical and modeling approaches have limitations. Empirical approaches are hampered by the relatively short duration of the climate record, the confounding of influences from various forcing mechanisms, and possible non-physical inconsistencies in the climate record that can result from changing monitoring techniques and analysis procedures (see Chapter 2 for examples of non-physical trends in precipitation due to shifts in reanalysis methods). The climate models are hampered by uncertainties in the representation of physical processes and by coarse spatial resolution, meaning that each grid cell in a global climate model generally covers an area of several hundred kilometers, which can lead to model biases.

In each case, the identified signal (forcing-response relationship) must be robust to these uncertainties, and requires demonstrating that an empirical analysis is both physically meaningful, is insensitive to sample size, and is reproducible when using different climate models. Best attribution practices employ combinations of empirical and numerical approaches using multiple climate models to minimize the effects of possible biases resulting from a single line of approach. Following this approach, Table 3.1 and Table 3.2 lists the observational and model datasets used to generate analyses in Chapter 3.

The specific attribution method can also differ according to the forcing-response relation being probed. As discussed below, three methods have been widely employed. These methods consider different hierarchical links in causal relationships as illustrated in the Figure 3.1 schematic and discussed in Section 3.1.2.1: (1) climate conditions arising from mechanisms internal to the atmosphere; (2) climate conditions forced from changes in atmospheric lower boundary conditions (for example, changes in ocean or

land surface conditions); and (3) climate conditions forced externally, whether natural or anthropogenic. In some cases, more than one of these links, or pathways, can be involved. For example, changes in greenhouse gas forcing may induce changes in the ocean component of the climate system. These changing ocean conditions can then force a response in the atmosphere that leads to regional temperature or precipitation changes.

3.1.2.1 Signal Determination

1) Attribution to internal atmospheric variations

Pioneering empirical research, based only on surface information, discovered statistical linkages between anomalous climate conditions that were separated by continents and oceans (Walker and Bliss, 1932), structures that are referred to today as teleconnection patterns. The North Atlantic Oscillation (NAO), which is a see-saw in anomalous pressure between the subtropical North Atlantic and the Arctic, and the Pacific-North American (PNA) pattern, which is a wave pattern of anomalous climate conditions arching across the North Pacific and North American regions, are particularly relevant to understanding North American climate variations. Chapter 2 illustrates the use of reanalysis data to diagnose the tropospheric wintertime atmospheric circulations associated with a specific phase of the PNA and NAO patterns, respectively. They each have widespread impacts on North American climate conditions as shown by station-based analyses of surface temperature and precipitation anomalies, and the reanalysis data of free atmospheric conditions provides the foundation for a physical explanation of the origins of those fingerprints (physical patterns), (see Section 3.1.2.2). The reanalysis data are also used to validate the realism of atmospheric circulation in climate models, as illustrated in Box. 3.1.

Observations of atmospheric circulation patterns in the free atmosphere fueled theories of the dynamics of these teleconnections, clarifying the origins for their regional surface impacts (Rossby, 1939). The relevant atmospheric circulations represent fluctuations in the semi-permanent positions of high and low pressure centers, their displacements being induced by a variety of mechanisms including

Table 3.2 Datasets utilized in the Product. The versions of these data used in this Product include data through December 2006. The web sites listed below provide URLs to the latest versions of these datasets, which may incorporate changes made after December 2006.

URL Link Information for Data Sets
CRU HadCRUT3v Climatic Research Unit of the University of East Anglia and the Hadley Centre of the UK Met Office
<http://www.cru.uea.uk/cru/data/temperature/>
NOAA Land/Sea Merged Temperature NOAA's National Climatic Data Center (NCDC)
<http://www.ncdc.noaa.gov/oa/climate/research/anomalies/>
NASA Land+Ocean Temperature NASA's Goddard Institute for Space Studies (GISS)
<http://data.giss.noaa.gov/gistemp/>
NCDC Gridded Land Temperature NOAA's National Climatic Data Center (NCDC)
Gridded Land Precipitation
<http://www.ncdc.noaa.gov/oa/climate/research/ghcn/>
NCDCdiv Contiguous U.S. Climate Division Data (temperature and precipitation)
<http://www.ncdc.noaa.gov/oa/climate/onlineprod/>
PRISM Spatial Climate Gridded Data Sets (temperature and precipitation) Oregon State University's Oregon Climate Service (OCS)
<http://prism.oregonstate.edu>
CHEN Global Land Precipitation NOAA's Climate Prediction Center (CPC)
<http://www.cpc.noaa.gov/products/precip/>
GPCC Global Gridded Precipitation Analysis Global Precipitation Climatology Centre (GPCC)
<http://www/dwd/de/en/FundE/Klima/KLIS/int/GPCC/>
CMIP3 CMIP3 World Climate Research Programme's (WCRP's) Coupled Model Intercomparison Project phase 3 (CMIP3) multi-model dataset
<http://www-pcmdi.llnl.gov/ipcc/>
Reanalysis NCEP50 National Centers for Environmental Prediction (NCEP), NOAA, and the National Center for Atmospheric Research (NCAR)
<http://dss.ucar.edu/pub/reanalysis/data_usr.html/>
ECHAM4.5 ECHAM4.5
<http://iridl.ldeo.columbia.edu/SOURCES/.IRI/.FD/.ECHAM4p5/.History/.MONTHLY>
NASA/NSIPP Runs

anomalous atmospheric heating (*e.g.*, due to changes in tropical rainfall patterns), changes in wind flow over mountains, the movement and development of weather systems (*e.g.*, along their storm tracks across the oceans), and other processes (Wallace and Guzzler, 1981; Horel and Wallace, 1981; see Glantz *et al.*, 1991 for a review of the various mechanisms linking worldwide climate anomalies). The PNA and NAO patterns are now recognized as representing preferred structures of extratropical climate variations that are readily triggered by internal atmospheric mechanisms and also by surface boundary variations, especially from ocean sea surface temperatures (Hoskins and Karoly, 1981; Horel and Wallace, 1981; Simmons *et al.*, 1983).

North American climate variations are often due to particular atmospheric circulation patterns that connect climate anomalies over distant regions of the globe.

As indicated in Chapter 2, these and other teleconnection patterns can be readily identified in the monthly and seasonal averages of atmospheric circulation anomalies in the free atmosphere using reanalysis data. Reanalysis data has also been instrumental in understanding the causes of teleconnection patterns and their North American surface climate impact (Feldstein 2000, 2002; Thompson and Wallace, 1998, 2000a,b). The ability to assess the relationships between teleconnections and their surface impacts provides an important foundation for attribution—North American climate variations are often due to particular atmospheric circulation patterns that connect climate anomalies over distant regions of the globe. Such a connection is illustrated schematically in Figure 3.1.

2) Attribution to surface boundary forcing

In some situations, teleconnections, including those described above, are a forced response to anomalous conditions at the Earth's surface. Under such circumstances, attribution statements that go beyond the statement of how recurrent features of the atmospheric circulation affect North American surface climate are feasible, and provide an explanation of the cause for the circulation itself. For instance, the atmospheric response to tropical Pacific sea surface temperature anomalies takes the form of a PNA-like pattern having significant impacts on North American climate, especially in the winter and spring seasons. However, other surface forcings, such as those related to sea ice and soil moisture conditions, can also cause appreciable climate anomalies, although their influence is more local and does not usually involve teleconnections.

Bjerknes (1966, 1969) demonstrated that a surface pressure see-saw between the western and eastern tropical Pacific (now known as the Southern Oscillation) was linked with the occurrence of equatorial Pacific sea surface temperature (SST) anomalies, referred to as El Niño. This so-called El Niño-Southern Oscillation (ENSO) phenomenon was discovered to be an important source for year-to-year North American climate variation, with recent examples being the strong El Niño events of 1982 to 1983 and 1997 to 1998, whose major meteorological consequences over North America included flooding and storm damage over a wide portion of the western and southern United States and unusually warm winter temperatures over the northern United States (Rasmusson and Wallace, 1983). The cold phase of the cycle, referred to as La Niña, also has major impacts on North America, in particular, an enhanced drought risk across the southern and western United States (Ropelewski and Halpert, 1986; Cole *et al.*, 2002).

The impacts of ENSO on North American climate have been extensively documented using both historical data and sensitivity experiments in which the SST conditions associated with ENSO are specified in atmospheric climate models (see review by Trenberth *et al.*, 1998). Figure 3.2 illustrates the observed wintertime tropospheric circulation pattern during El Niño events of the last half century based on reanalysis data, and the associated North American surface signatures in temperature and precipitation. Reanalysis data is accurate enough to distinguish between the characteristic circulation pattern of the PNA (Figure 2.8) and that induced by ENSO—the latter having more widespread high pressure over Canada. Surface temperature features consist more of a north-south juxtaposition of warm-cold over North America during ENSO, as compared to the west-east structure associated with the PNA. The capacity to observe such distinctions is important when determining attribution because particular climate signatures indicate different possible causes.

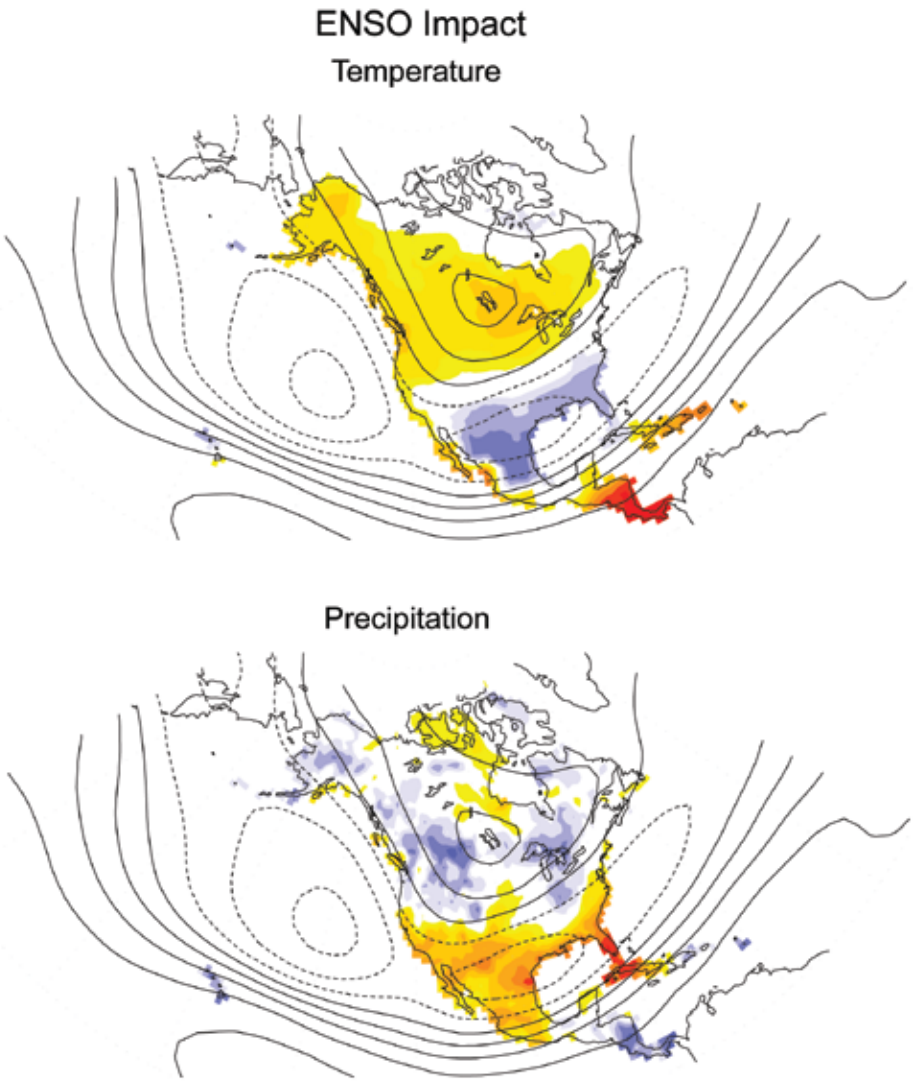

El Niño is a known internal variation of the coupled ocean-atmosphere.

Figure 3.2 The correlation between a sea surface temperature index of El Niño-Southern Oscillation (ENSO) and 500 millibar (mb) pressure height field (contours). The shading indicates the correlations between ENSO index and the surface temperature (top panel) and the precipitation (bottom panel). The 500mb height is from the NCEP/NCAR R1 reanalysis. The surface temperature and precipitation are from independent observational datasets. The correlations are based on seasonal mean winter (December-January-February) data for the period 1951 to 2006. The contours with negative correlation are dashed.

The use of climate models subjected to specified SSTs has been essential for determining the role of oceans in climate, and such tools are now extensively used in seasonal climate forecast practices. The atmospheric models are often subjected to realistic globally complete, monthly evolving SSTs (so-called AMIP experiments [Gates, 1992]) or to regionally confined idealized SST anomalies in order to explore specific cause-effect relations. These same models have also been used to assess the role of sea ice and soil moisture conditions on climate.

The process of forcing a climate model is discussed further in Box 3.2.

3) Attribution to external forcing

Explaining the origins for the surface boundary conditions themselves is another stage in attribution. El Niño, for example, is a known internal variation of the coupled ocean-atmosphere. On the other hand, a warming trend of ocean SST, as seen in recent decades over the tropical warm pool of the Indian Ocean/West Pacific, is recognized to result in part from changes in greenhouse gas forcing (Santer *et*

BOX 3.2: Forcing a Climate Model

The term "forcing" as used in Chapter 3 refers to a process for subjecting a climate model to a specified influence, often with the intention to probe cause-effect relationships. The imposed conditions could be "fixed" in time, such as a might be used to represent a sudden emission of aerosols by volcanic activity. It may be "time evolving" such as by specifying the history of sea surface temperature variations in an atmospheric model. The purpose of forcing a model is to study the Earth system response, and the degrees of freedom sensitivity of that response to both the model and the forcing employed. The schematic of the climate system helps to better understand the forcings used in various models of Chapter 3.

For atmospheric model simulations used in this SAP, the forcing consists of specified monthly evolving global sea surface temperatures during 1951 to 2006. By so restricting the lower boundary condition of the simulations, the response of unconstrained features of the climate system can be probed. In this SAP, the atmosphere and land surface are free to respond. Included in the former are the atmospheric hydrologic cycle involving clouds, precipitation, water vapor, temperature, and free atmospheric circulation. Included in the latter is soil moisture and snow cover, and changes in these can further feedback upon the atmosphere. Sea ice has been specified to climatological conditions in the simulations of this report, as has the chemical composition of the atmosphere including greenhouse gases, aerosols, and solar output.

For coupled ocean-atmosphere model simulations used in this SAP, the forcing consists of specified variations in atmospheric chemical composition (*e.g.,* carbon dioxide, methane, nitrous oxide), solar radiation, volcanic and anthropogenic aerosols. These are estimated from observations during 1951 to 2000, and then based upon a emissions scenario for 2001 to 2006. The atmosphere, land surface, ocean, and sea ice are free to respond to these specified conditions. The atmospheric response to those external forcings could result from the altered radiative forcing directly, though interactions and feedbacks involving the responses of the lower boundary conditions (*e.g.*, oceans and cryosphere) are often of leading importance. For instance, much of the high-latitude amplification of surface air temperature warming due to greenhouse gas emissions is believed to result from such sea ice and snow cover feedback processes. Neither the coupled ocean-atmospheric models nor the atmospheric models used in this SAP include changes in land surface, vegetation, or ecosystems. Nor does the oceanic response in the coupled models include changes in biogeochemistry.

Multiple realizations of the climate models subjected to the same forcings are required in order to effectively separate the climate model's response from low-frequency climate variability. Ensemble methods are therefore used in Chapter 3. In the case of the atmospheric models, 33 total simulations (derived from two different models) forced as discussed above are studied. In the case of the coupled ocean-atmosphere models, 41 total simulations (derived from 19 different models) forced as discussed above are studied

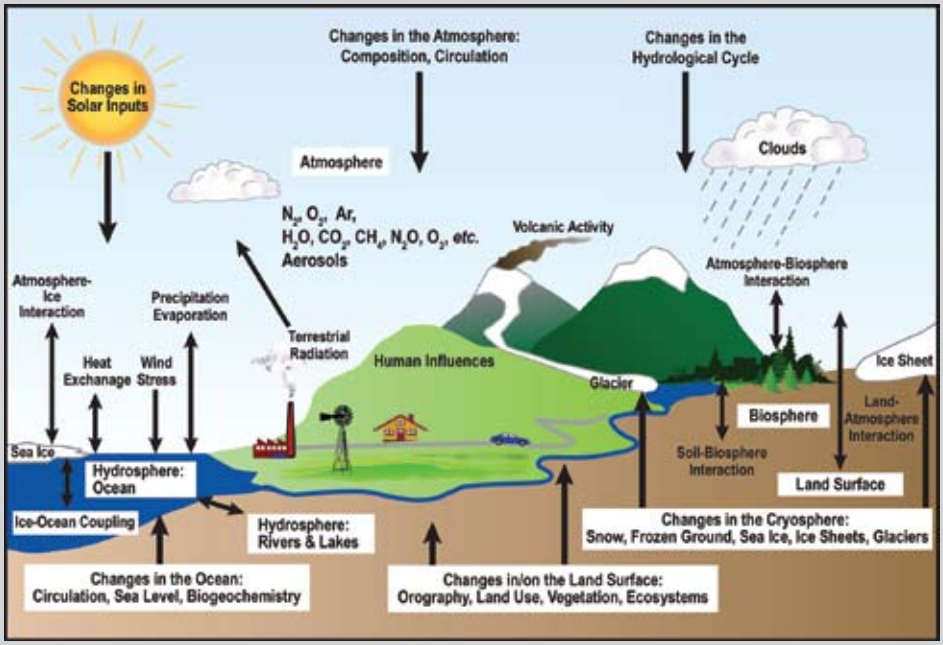

Figure Box 3.2 Schematic view of the components of the climate system, their processes and interactions (From IPCC, 2007a).

al., 2006; Knutson *et al.*, 2006). Figure 3.1 highlights the differences in how SSTs vary over the eastern *versus* western tropical Pacific as a consequence of different processes occurring in those regions. Thus, the remote effects of recent sea surface warming of the tropical ocean's warmest waters (the so-called warm pool) on North American climate might be judged to be of external origins to the ocean-atmosphere system, tied in part to changes in the atmosphere's chemical composition.

The third link in the attribution chain involves attribution of observed climate conditions to external forcing. The external forcing could be natural, for instance originating from volcanic aerosol effects or solar fluctuations, or the external forcing could be anthropogenic. As discussed extensively in the IPCC Reports, the attribution of climate conditions to external radiative forcing (greenhouse gases, solar, and volcanic forcing) can be done directly by specifying the natural and anthropogenic forcings within coupled ocean-atmosphere-land models. An indirect approach can also be used to attribute climate conditions to external forcing, for instance, probing the response of an atmospheric model to SST conditions believed to have been externally forced (Hoerling *et al.*, 2004). However, if an indirect approach is used, it can only be *qualitatively* determined that external forcing contributed to the event—an accurate *quantification* of the magnitude of the impact by external forcing can only be determined in a direct approach.

The tool used for attribution of external forcing, either to test the signal (see Section 3.1.2.2) due to anthropogenic greenhouse gas and atmospheric aerosol changes or land use changes, or natural external forcing due to volcanic and solar forcing, involves coupled ocean-atmosphere-land models forced by observed external forcing variations. As illustrated in Figure 3.1, this methodology has been widely used in the IPCC Reports to date. Several studies have used reanalysis data to first detect change in atmospheric circulation, and then test with models whether such change resulted from human influences. (Chapter 2 also discusses the use of reanalysis data in establishing the suitability of climate models used for attribution.) For instance, a trend in wintertime sea level pressure has been observed and confirmed in reanalysis data that resembles the positive polarity of the NAO (high surface pressure over the midlatitude North Atlantic and low pressure over the Arctic), and greenhouse gas and sulfate aerosol changes due to human activities have been implicated as a contributing factor (Gillett *et al.*, 2003; Figure 3.7). Reanalysis data have been used to detect an increase in the height of the tropopause—a boundary separating the troposphere and stratosphere—and modeling results have established anthropogenic changes in stratospheric ozone and greenhouse gases as the primary cause (Santer *et al.*, 2003).

3.1.2.2 Fingerprinting

Many studies use climate models to predict the expected pattern of response to a forcing, referred to as "fingerprints" in the classic climate change literature, or more generally referred to as the "signal" (Mitchell *et al.*, 2001; IDAG, 2005; Hegerl *et al.*, 2007). The space and time scales used to analyze climate conditions are typically chosen so as to focus on the space and time scale of the signal itself, filtering out structure that is believed to be unrelated to forcing. For example, changes in greenhouse gas forcing are expected to cause a large-scale (global) pattern of warming that evolves slowly over time, and thus scientists often smooth data to remove small-scale variations in both time and space. On the other hand, it is expected that ENSO-related SST forcing yields a regionally focused pattern over the Pacific North American sector, having several centers of opposite signed anomalies (*i.e.*, warming or cooling), and therefore averaging over a large region such as this is inappropriate. To ensure that a strong signal has been derived from climate models, individual realizations of an ensemble, in which each member has been identically forced, are averaged. Ensemble methods are thus essential in separating the model's forced signal from its internal variability so as to minimize the mix of signal and noise, which results from unforced climatic fluctuations.

Many studies use climate models to predict the expected pattern of response to a forcing, referred to as "fingerprints" in the classic climate change literature, or more generally referred to as the "signal".

The consistency between an observed climate condition and the estimated response to a hypothesized key forcing is determined by (1) estimating the amplitude of the expected fingerprint empirically from observations; (2) assessing whether this estimate is statistically

consistent with the expected amplitude derived from forced model experiments; and then (3) inquiring whether the fingerprint related to the key forcing is distinguishable from that due to other forcings. The capability to do this also depends on the amplitude of the expected fingerprint relative to the noise.

In order to separate contributions by different forcings and to investigate if other combinations of forcing can also explain an observed event, the simultaneous effect of multiple forcings are also examined, typically using a statistical multiple regression analysis of observations onto several fingerprints representing climate responses to each forcing that, ideally, are clearly distinct from one another (Hasselmann, 1979; 1997; Allen and Tett, 1999; IDAG, 2005; Hegerl *et al.*, 2007). Examples include the known unique sign and global patterns of temperature response to increased sulfate aerosols (cooling of the troposphere, warming of the stratosphere) *versus* increased carbon dioxide (warming of the troposphere but cooling of the stratosphere). Another example is the known different spatial patterns of atmospheric circulation response over the North American region to SST forcing from the Indian Ocean compared to the tropical eastern Pacific Ocean (Simmons *et al.*, 1983; Barsugli and Sardeshmukh, 2002). If the climate responses to these key forcings can be distinguished, and if rescaled combinations of the responses to other forcings fail to explain the observed change, then the evidence for a causal connection is substantially increased. Thus, the attribution of recent large-scale warming to greenhouse gas forcing becomes more reliable if influences of other natural external forcings, such as solar variability, are explicitly accounted for in the analysis.

The attribution of recent large-scale warming to greenhouse gas forcing becomes more reliable if influences of other natural external forcings, such as solar variability, are explicitly accounted for in the analysis.

The confidence in attribution will thus be subject to the uncertainty in the fingerprints both estimated empirically from observations and numerically from forced model simulations. The effects of forcing uncertainties, which can be considerable for some forcing variables such as solar irradiance and aerosols, also remain difficult to evaluate despite recent advances in research.

Satellite and *in situ* observations during the reanalysis period yield reliable estimates of SST conditions over the world oceans, thus increasing the reliability of attribution based on SST forced atmospheric models. Estimates of other land surface conditions, including soil moisture and snow cover, are less reliable. Attribution results based on several models or several forcing observation histories also provide information on the effects of model and forcing uncertainty. Likewise, empirical estimates of fingerprints derived from various observational datasets provide information of uncertainty.

Finally, attribution requires knowledge of the internal climate variability on the time scales considered—the noise within the system against which the signal is to be detected and explained. The residual (remaining) variability in instrumental observations of the Earth system after the estimated effects of external forcing (*e.g.*, greenhouse gases and aerosols) have been removed is sometimes used to estimate internal variability of the coupled system. However, these observational estimates are uncertain because the instrumental records are too short to give a well-constrained estimate of internal variability, and because of uncertainties in the forcings and the corresponding estimates of responses. Thus, internal climate variability is usually estimated from long control simulations from climate models. Subsequently, an assessment is usually made of the consistency between the residual variability referred to above and the model-based estimates of internal variability; and analyses that yield implausibly large residuals are not considered credible. Confidence is further increased by comparisons between variability in observations and climate model data, by the ability of models to simulate modes of climate variability, and by comparisons between proxy reconstructions and climate simulations of the last millennium.

Sections 3.2, 3.3, 3.4, and 3.5 summarize current understanding on the causes of detected changes in North American climate. These sections will illustrate uses of reanalysis data in combination with surface temperature and precipitation measurements to examine the nature of North American climate variations, and compare with forced model experiments that test attributable causes. In addition, these sections also assess the current understanding of causes for other variations of significance

in North America's recent climate history, focusing especially on major North American droughts. In the mid-1930s, Congress requested that the Weather Bureau explain the causes for the 1930s Dust Bowl drought, with a key concern being to understand whether this event was more likely a multi-year occurrence or an indication of longer-term change. Similar to 70 years earlier, fundamental challenges in attribution science today are to distinguish quasi-cyclical variations from long-term trends, and natural from anthropogenic origins.

3.2 PRESENT UNDERSTANDING OF NORTH AMERICAN ANNUAL TEMPERATURE AND PRECIPITATION CLIMATE TRENDS FROM 1951 TO 2006

3.2.1 Summary of IPCC Fourth Assessment Report

Among the major findings of the IPCC Fourth Assessment Report (IPCC, 2007b) is that "it is *likely* that there has been significant anthropogenic warming over the past 50 years averaged over each continent except Antarctica". This conclusion was based on recent fingerprint-based studies on the attribution of annual surface temperature involving space-time patterns of temperature variations and trends. Model studies using only natural external forcings were unable to explain the warming over North America in recent decades, and only experiments including the effects of anthropogenic forcings reproduced the recent upward trend. The IPCC Report also stated that, for precipitation, there was low confidence in detecting and attributing a change, especially at the regional level.

This assessment focuses in greater detail on North American temperature and precipitation variability during the period 1951 to 2006.

The origins for the North American fluctuations are assessed by examining the impacts on North America from time-evolving sea surface conditions (including ENSO and decadal ocean variations), in addition to time evolving anthropogenic effects. The use of reanalysis data to aid in the attribution of surface climate conditions is illustrated.

3.2.2 North American Annual Mean Temperature

3.2.2.1 Description of the Observed Variability

Seven of the warmest ten years since 1951 have occurred in the last decade (1997 to 2006). The manner in which North American annual temperatures have risen since 1951, however, has been neither smooth nor consistent, being characterized by occasional peaks and valleys (Figure 3.3, top). The coldest year since 1951 occurred in 1972, and below average annual temperatures occurred as recently as 1996. Explanations for such substantial variability are no less important than explanations for the warming trend.

Seven of the warmest ten years since 1951 have occurred in the last decade (1997 to 2006). Virtually all of the warming averaged over North America since 1951 has occurred after 1970.

Virtually all of the warming averaged over North America since 1951 has occurred after 1970. It is noteworthy that North American temperatures cooled during the period 1951 through the early 1970s. In the 1970s, the general public and policy makers were interested in finding the reason for this cooling, with concerns about food production and societal disruptions. They turned to the meteorological community for expert assessment. Unfortunately, climate science was in its early stages and attribution was considerably more art than science. The essential tools for performing rigorous attribution such as global climate models were not yet available, nor was much known then about the range of historical climate variations such as those that have been subsequently revealed by paleoclimate studies. A consistent climate analysis of the historical instrumental record that included descriptions of the free atmosphere was also unavailable.

Barring an explanation of the cause for the cooling, and with no comprehensive climate models available, some scientists responded to the public inquiries on what would happen by merely extrapolating recent trends, thereby portraying an increased risk for a cooling world (Kukla and Mathews, 1972). Others suggested in the mid-1970s that we might be at the brink of a pronounced global warming, arguing that internal variations of the climate were then masking an anthropogenic signal (Broecker, 1975). The 1975 National Academy of Sciences report (NRC, 1975) on understanding climate change emphasized the fragmentary state of knowledge

BOX 3.3: Choosing the Assessment Period

The authors of this Product were asked to examine the strengths and limitations of current reanalysis products, and to assess capabilities for attributing the causes for climate variations and trends during the reanalysis period. The scope of this assessment is thus bounded by the reanalysis record (1948 to present). An important further consideration is the availability of sufficient, quality controlled surface observations to define key climate variations accurately. For precipitation, a high quality global gridded analysis is available beginning in 1951, thereby focusing the attribution to the period from 1951 to 2006.

It is reasonable to ask whether such a 56-year assessment period adequately samples the principal features of climate variability. Does it, for example, capture the major climate events, such as droughts, that may be of particular concern to decision makers? Is it a sufficiently long period to permit the distinction between fluctuations in climate conditions that are transient, or cyclical, from trends that are related to a changing climate? How well do scientists understand the climate conditions prior to 1951, and what insight does analysis of those conditions provide toward explaining post-1950 conditions? These are all important questions to bear in mind when reading this Product, especially if one wishes to generalize conclusions about the nature of and causes for climate conditions during 1951 to 2006 to earlier or future periods.

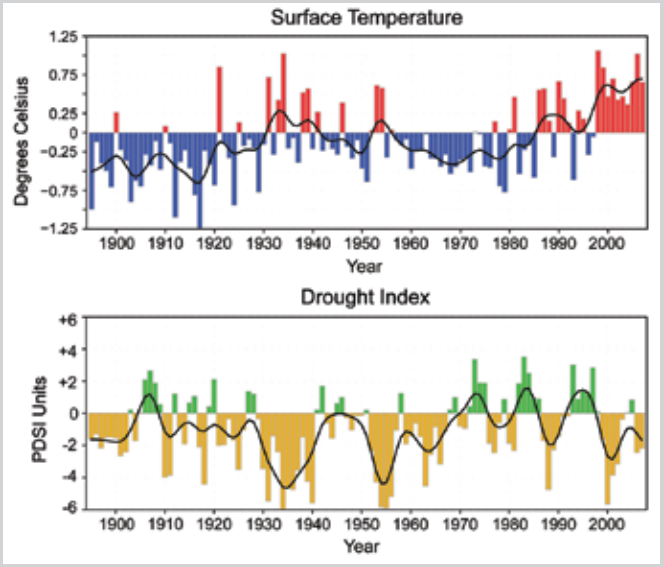

Figure Box 3.3 Time series of U.S. area-averaged and annually averaged surface air temperature (top) and the Palmer Drought Severity Index (bottom) for the period 1895 to 2006. Curves are smoothed annual values using a nine-point Gaussian filter. The Gaussian filter is a weighted time averaging applied to the raw annual values in order to highlight lower frequency variations. "Nine-point" refers to the use of nine annual values in the weighting process. Data source is the contiguous U.S. climate division data of NOAA's National Climatic Data Center.

As a case in point, the U.S. surface temperature record since 1895 is remarkable for its multi-decadal fluctuations (top panel). A simple linear trend fails to describe all features of U.S. climate variations, and furthermore, a trend analysis for any subset of this 112-year period may be problematic since it may capture merely a segment of a transient oscillation. The 1930s was a particularly warm period, one only recently eclipsed. The United States has undergone two major swings between cold epochs (beginning in the 1890s and 1960s) and warm epochs (1930s and 2000s). It is reasonable to wonder whether the current warmth will also revert to colder conditions in coming decades akin to events following the 1930s peak, and attribution science is therefore important for determining whether the same factors are responsible for both warmings or not. Some studies reveal that the earlier warming may have resulted from a combination of anthropogenic forcing and an unusually large natural multi-decadal fluctuation of climate (Delworth and Knutson, 2000). Other work indicates a contribution to the early twentieth century warming by natural forcing of climate, such as changes in solar radiation or volcanic activity (*e.g.*, Hegerl *et al.*, 2006). The 1930s warming was part of a warming focused mainly in the northern high latitudes, a pattern reminiscent of an increase in poleward ocean heat transport (Rind and Chandler, 1991), which can itself be looked upon as due to "natural variability". In contrast, the recent warming is part of a global increase in temperatures, and the IPCC Fourth Assessment Report, Chapter 9 states that it is likely that a significant part of warming over the past 50 years over North America may be human related (IPCC, 2007a), thus contrasting causes of the warming that occurred in this period from that in 1930s. The physical processes related to this recent warming are further examined in this Chapter.

The year 1934 continues to stand out as one the warmest years in the United States' 112-year record, while averaged over the entire globe, 1934 is considerably cooler than the recent decade. The warmth of the United States in the 1930s coincided with the Dust Bowl (lower panel), and drought conditions likely played a major role in increasing land surface temperatures. Prior studies suggest that the low precipitation during the Dust Bowl was related in part to sea surface temperature conditions over the tropical oceans (Schubert *et al.*, 2004; Seager *et al.*, 2005). Current understanding of severe U.S. droughts that have occurred during the reanalysis period as described in this Chapter builds upon such studies of the Dust Bowl.

of the mechanisms causing climate variations and change, and posed the question of whether scientists would be able to recognize the first phases of a truly significant climate change when it does occur (NRC, 1975). Perhaps the single most important attribution challenge today regarding the time series of Figure 3.3 is whether the reversal of the cooling trend after 1975 represents such a change, and one for which a causal explanation can be offered.

There is very high confidence in the detection that the observed temperature trend reversed after the early 1970s. The shaded area in Figure 3.3 (top right panel) illustrates the spread among four different analyses of surface measurements (see Table 3.2 for descriptions of these data), and the analysis uncertainty as revealed by their range is small compared to the amplitude of the trend and principal variations. Also shown is the surface temperature time series derived from the reanalysis. Despite the fact that the assimilating model used in producing the NCEP/NCAR reanalysis does not incorporate observations of surface temperature (Kalnay *et al.*, 1996), the agreement with the *in situ* observations is strong. This indicates that the surface temperature averaged over the large domain of North America is constrained by and is consistent with climate conditions in the free atmosphere. Both for the emergent warming trend in the 1970s, and for the variations about it, this excellent agreement among time series based on different observational datasets and the reanalysis increases confidence that they are not artifacts of analysis procedure.

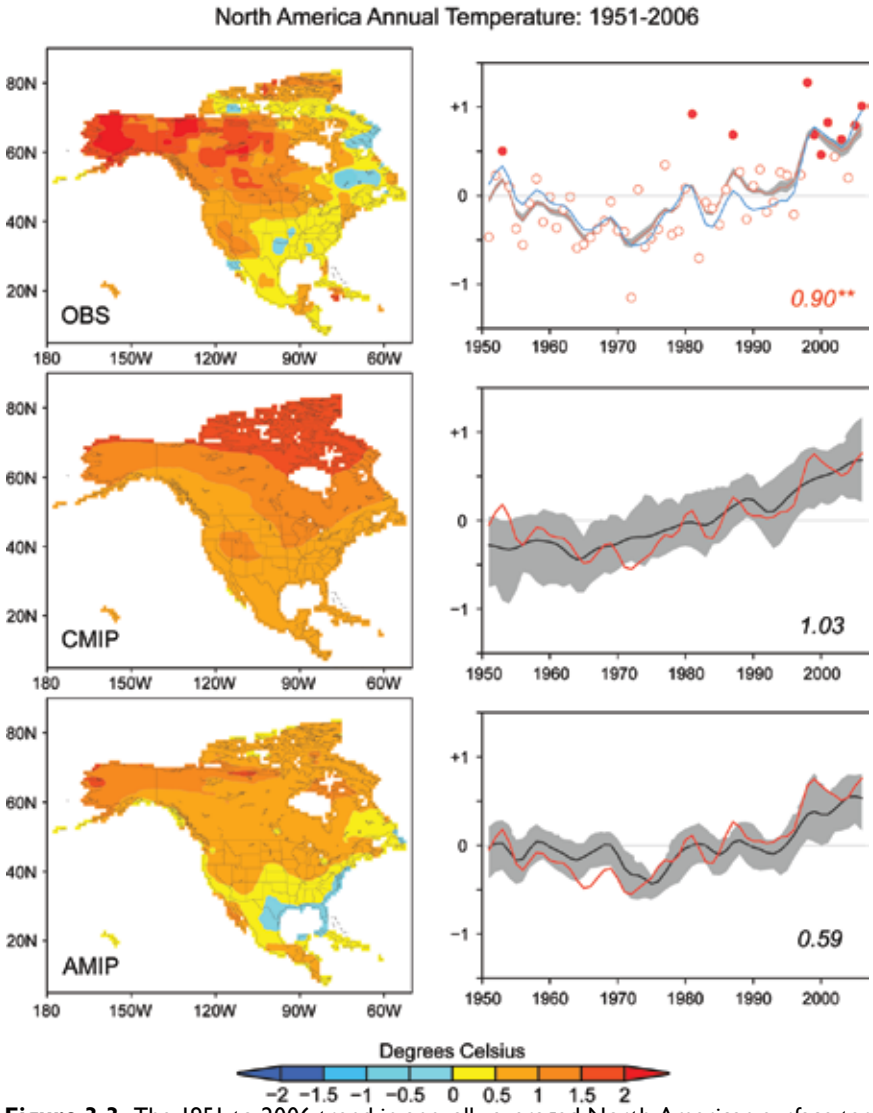

Figure 3.3 The 1951 to 2006 trend in annually averaged North American surface temperature from observations (top), CMIP simulations (middle), AMIP simulations (bottom). Maps (left side) show the linear trend in annual temperatures for 1951 to 2006 (units, °C change over 56 years). Time series (right side) show the annual values from 1951 to 2006 of surface temperatures averaged over the whole of North America. Curves are smoothed annual values using a five-point Gaussian filter, based on the average of four gridded surface observational analyses, and the ensemble mean of climate simulations. The Gaussian filter is a weighted time-averaging applied to the raw annual values in order to highlight lower frequency variations. "Five-point" refers to the use of five annual values in the weighting process. Unsmoothed annual observed temperatures are shown by red circles, with filled circles denoting the ten warmest years since 1951. Plotted values are the total 56-year change (°C), with the double asterisks denoting very high confidence that an observed change was detected. For observations, the gray band denotes the range among four surface temperature analyses. The blue curve is the NCEP/NCAR reanalysis surface temperature time series. For simulations, the gray band contains the 5 to 95 percent occurrence of individual model simulations.

The total 1951 to 2006 change in observed North American annual surface temperatures is +0.90°C ± 0.1°C (about +1.6°F ± 0.2°F), with the uncertainty estimated from the range between trends derived from four different observational analyses. Has a *significant* North American warming been detected? Answers to this question require knowledge of the plausible range in 56-year trends that can occur naturally in the absence of any time varying anthropogenic forcing. The length of the observational record does not permit such an assessment, but an analysis of such variations in coupled model simulations that exclude variations in anthropogenic forcing provides an indirect estimate. To estimate the confidence that a change in

Numerous detection and attribution studies have shown that the observed warming of North American surface temperature since 1950 cannot be explained by natural climate variations. alone and is consistent with the response to anthropogenic climate forcing, particularly increases in atmospheric greenhouse gases

North American temperatures has been detected, a non-parametric test, which makes no assumptions about the statistical distribution of the data, has been applied that estimates the range of 56-year trends attributable to natural variability alone (see Appendix B for methodological details). A diagnosis of 56-year trends from the suite of "naturally forced" Coupled Model Intercomparison Project (CMIP) runs is performed, from which a sample of 76 such trends were generated for annual North American average surface temperatures. Of these 76 "trends estimates" consistent with natural variability, no single estimate was found to generate a 56-year trend as large as observed.

It is thus *very likely* that a change in North American annual mean surface temperature has been detected. That assessment takes into account the realization that the climate models have biases that can affect statistics of their simulated internal climate variability.

3.2.2.2 Attribution of the Observed Variations

3.2.2.2.1 External Forcing

The IPCC Fourth Assessment Report provided strong attribution evidence for a significant anthropogenic greenhouse gas forced warming of North American surface temperatures (IPCC, 2007a). Figure 3.4 is drawn from that Report, and compares continental-averaged surface temperature changes observed with those simulated using the CMIP coupled models having both natural and anthropogenic forcing. It is clear that only experiments using observed time varying anthropogenic forcing explain the warming in recent decades. Numerous detection and attribution studies, as reviewed by Hegerl *et al.* (2007), have shown that the observed warming of North American surface temperature since 1950 cannot be explained by natural climate variations alone and is consistent with the response to anthropogenic climate forcing, particularly increases in atmospheric greenhouse gases (Karoly *et al.*, 2003; Stott, 2003; Zwiers and Zhang, 2003; Knutson *et al.*, 2006; Zhang *et al.*, 2006). The suitability of these coupled climate models for attribution is indicated by the fact that they are able to simulate variability on time scales of decades and longer that is consistent with reanalysis data of the free atmosphere and surface observations over North America (Hegerl *et al.*, 2007).

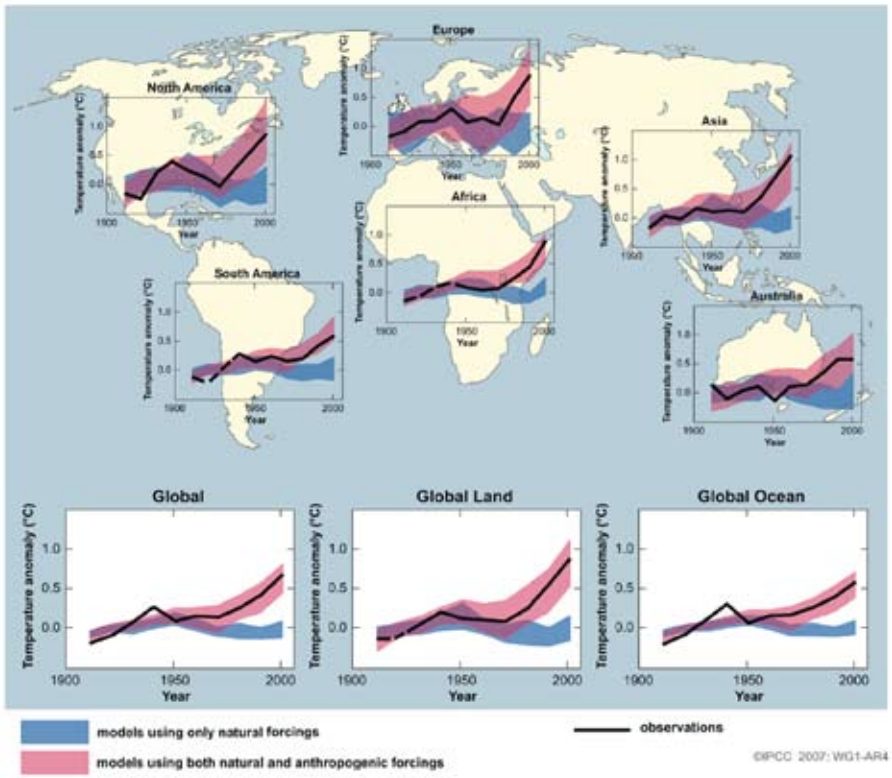

Figure 3.4 Temperature changes relative to the corresponding temperature average for 1901 to 1950 (°C) from decade to decade for the period 1906 to 2005 over the Earth's continents, as well as the entire globe, global land area, and the global ocean (lower graphs). The black line indicates observed temperature change and the colored bands show the combined range covered by 90 percent of recent model simulations. Red indicates simulations that include natural and human factors, while blue indicates simulations that include only natural factors. Dashed black lines indicate decades and continental regions for which there are substantially fewer observations compared with other continents during that time. Detailed descriptions of this figure and the methodology used in its production are given in Hegerl *et al.* (2007).

A more detailed examination of the human influence on North America is provided in Figure 3.3 (middle) that shows the spatial map of the 1951 to 2006 model-simulated surface temperature trend, in addition to the trend over time. There are several key agreements between the CMIP simulations and observations that support the argument for an anthropogenic effect. First, both indicate that most of the warming has occurred in the past 30 years. The North American warming after 1970 is thus *likely* the result of the region's response to anthropogenic forcing. Second, the total 1951 to 2006 change in observed North American annual surface tem-

peratures of +0.90°C (about +1.6°F) compares well to the simulated ensemble averaged warming of +1.03°C (almost +1.9°F). Whereas the observed 56-year trend was shown in Section 3.2.2.1 to be inconsistent with the population of trends drawn from a state of natural climate variability, the observed warming is found to be consistent with the population of trends drawn from a state that includes observed changes in the anthropogenic greenhouse gas forcing during 1951 to 2006.

Further, the observed low frequency variations of annual temperature fall within the 5 to 95 percent uncertainty range of the individual model simulations. All CMIP runs that include anthropogenic forcing produce a North American warming during 1951 to 2006. For some simulations, the trend is less than that observed and for some it is greater than that observed. This range results from two main factors. One is the uncertainty in anthropogenic signals; namely that the individual 19 models subjected to identical forcing exhibit somewhat different sensitivities. The other results from the internal variability of the models; namely that individual runs of the same model generate a range of anomalies owing to natural coupled-ocean atmosphere fluctuations.

Each of the 41 anthropogenic forced simulations produces a 56-year North American warming (1951 to 2006) that accounts for more than half of the observed warming. Our assessment of the origin for the observed North American surface temperature trend is that more than half of the warming during 1951 to 2006 is *likely* the result of human influences. It is exceptionally *unlikely* that the observed warming has resulted from natural variability alone because there is a clear separation between the ensembles of climate model simulations that include only natural forcings and those that contain both anthropogenic and natural forcings (Hegerl *et al.*, 2007). These confidence statements reflect the uncertainty of the role played by model biases in their sensitivity to external forcing, and also the unknown impact of biases on the range of their unforced natural variability.

More than half of the warming over North America during 1951 to 2006 is *likely* the result of human influences. It is exceptionally *unlikely* that the observed warming has resulted from natural variability alone.

From Figure 3.3, it is evident that the yearly fluctuations in observed North American temperature are of greater amplitude than those occurring in the ensemble average of externally

BOX 3.4: Use of Expert Assessment

The use of expert assessment is a necessary element in attribution as a means to treat the complexities that generate uncertainties. Expert assessment is used to define levels of confidence, and the terms used in this Product (see Preface) follow those of the IPCC Fourth Assessment Report. The attribution statements used in Chapter 3 of this SAP also employ probabilistic language (for example, "virtually certain") to indicate a likelihood of occurrence.

To appreciate the need for expert assessment, it is useful to highlight the sources of uncertainty that arise in seeking the cause for climate conditions. The scientific process of attribution involves various tools to probe cause-effect relationships such as historical observations, climate system models, and mechanistic theoretical models. Despite ongoing improvements in reanalysis and models, these and other tools have inherent biases rendering explanations of the cause for a climate condition uncertain. Uncertainty can arise in determining a forced signal (*i.e.*, fingerprint identification). For instance, the aerosol-induced climate signal involves direct radiative effects that require on accurate knowledge of the amount and distribution of aerosols in the atmosphere. These are not well observed quantities, leading to so-called "value uncertainties" (IPCC, 2007a) because the forcing itself is poorly known. The aerosol-induced signal also involves an indirect radiative forcing, the latter depending on cloud properties and water droplet distributions. These cloud radiative interactions are poorly represented in current generation climate models (Kiehl, 1999), contributing to so-called "structural uncertainties" (IPCC, 2007a). Even if the forcing is known precisely and the model includes the relevant processes and relationships, the induced signal may be difficult to distinguish from other patterns of climate variability thereby confounding the attribution.

The scientific peer-reviewed literature provides a valuable guide to the author team of Chapter 3 for determining attribution confidence. In addition, new analyses in this Product are also examined in order to provide additional information. These employ methods and techniques that have been extensively tested and used in the scientific literature. In most cases, new analyses involve observational data and model simulations that have merely updated to include recent years through 2006.

The oceans play a major role in climate, not only for determining its average conditions and seasonal cycle, but also for determining its anomalous conditions including interannual-to-decadal fluctuations.

forced runs. This is consistent with the fact that the observations blend the effects of internal and external influences while the model estimates only the time-evolving impact of external forcings. Nonetheless, several of these observed fluctuations align well with those in the CMIP data. In particular, the model warming trend is at times punctuated by short periods of cooling, and these episodes coincide with major tropical volcanic eruptions (*e.g.*, Aguang in 1963; Mt. Pinatubo in 1991). These natural externally forced cooling episodes correspond well with periods of observed cooling, as will be discussed further in Section 3.4.

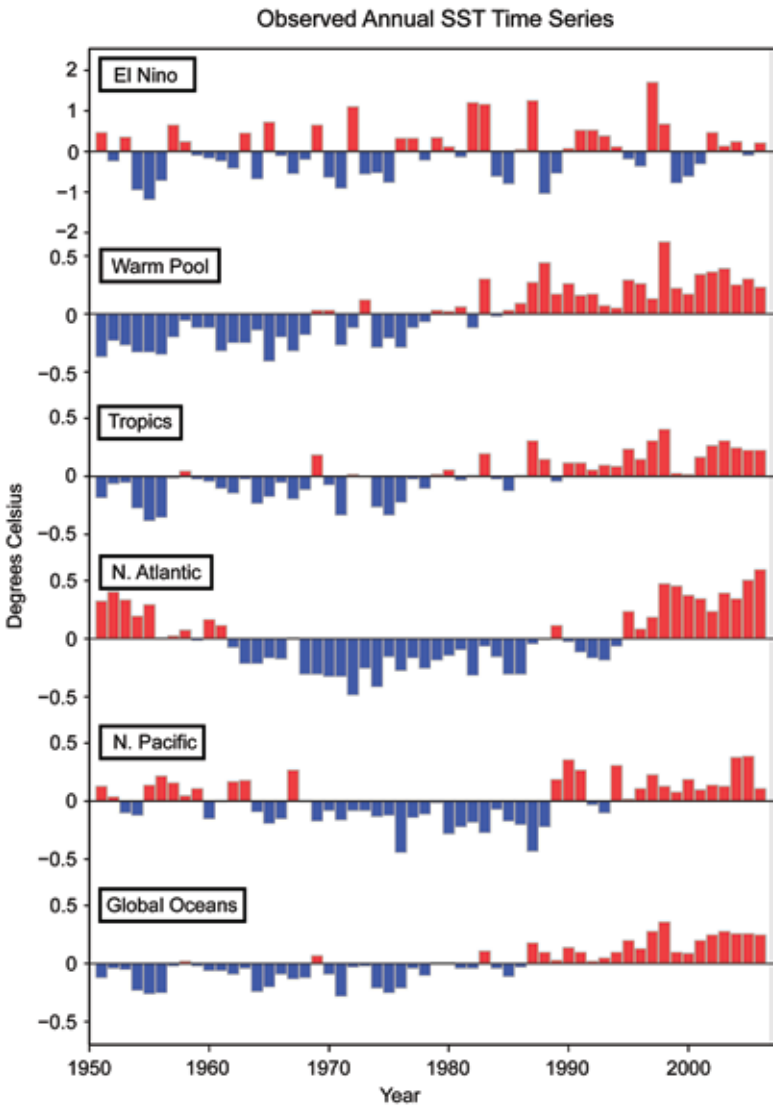

Figure 3.5 Observed annual mean sea surface temperature (SST) time series for 1951 to 2006. The oceanic regions used to compute the indices are 5°N to 5°S, 90°W to 150°W for El Niño, 10°S to 10°N, 60°E to 150°E for the warm pool, 30°S to 30°N for the tropics, 30°N to 60°N for the North Atlantic, 30°N to 60°N for the North Pacific, and 40°S to 60°N for the global oceans. The dataset used is the HadiSST monthly gridded fields, and anomalies are calculated relative to a 1951 to 2006 climatological reference.

3.2.2.2 Sea Surface Temperature Forcing

The oceans play a major role in climate, not only for determining its average conditions and seasonal cycle, but also for determining its anomalous conditions including interannual-to-decadal fluctuations. Section 3.1 discussed modes of anomalous sea surface temperature (SST) variations that impact North America, in particular those associated with ENSO. Figure 3.5 illustrates the variations in time of SSTs over the global oceans and over various ocean basins during 1951 to 2006. Three characteristic features of the observed SST fluctuations are noteworthy. First, SSTs in the eastern tropical Pacific (top panel) vary strongly from year to year, as warm events alternate with cold events, which is indicative of the ENSO cycle. Second, extratropical North Pacific and North Atlantic SSTs have strong year-to-year persistence, with decadal periods of cold conditions followed by decadal periods of warm conditions. Third, the warm pool of the tropical Indian Ocean/West Pacific, the tropically averaged SSTs, and globally averaged SSTs are dominated by a warming trend. In many ways, these resemble the North American surface temperature changes over time, including a fairly rapid emergence of warmth after the 1970s.

A common tool for determining the SST effects on climate is the use of atmospheric general circulation models (AGCM) forced with the specified time evolution of the observed SSTs, in addition to empirical methodologies (see Figure 3.2 for the El Niño impact inferred from reanalysis data, and Box 3.1 for an assessment of model simulated ENSO teleconnections). Such numerical modeling approaches are generally referred to as AMIP simulations (Gates, 1992), and that term is adapted in this Product to refer to model runs spanning the period 1951 to 2006.

Much of the known effect of SSTs has focused on the boreal winter season, a time when ENSO and its impacts on North America are at their peak. However, the influence of SSTs on annual average variability over North America is not yet documented in the peer-reviewed literature. Therefore, an expert assessment is presented in this Section based on the analysis of two AGCMs (Table 3.1). It is important to note that the AMIP simulations used in this analysis do

not include the observed evolution of external forcings (*e.g.*, solar, volcanic aerosols, or anthropogenic greenhouse gases). The specified SSTs may, however, reflect the footprints of such external influences (see Section 3.4 and Figure 3.18 for a discussion of the same SST time series constructed from the CMIP simulations).

North American annual temperature trends and their evolution over time are well replicated in the AMIP simulations (Figure 3.3, bottom). There are several key agreements between the AMIP simulations and observations that support the argument for an SST effect. First, most of the AMIP simulated warming occurs after 1970, in agreement with observations. The time evolution of simulated annual North American surface temperature fluctuations is very realistic, with a temporal correlation of 0.79 between the raw unsmoothed observed data and simulated annual values. While slightly greater than the observed correlation with CMIP of 0.68, much of the positive year-over-year correlation is due to the warming trend. Second, the AMIP pattern correlation of 0.87 with the observed trend map highlights the remarkable spatial agreement and exceeds the 0.79 spatial correlation for the CMIP simulated trend. Several other notable features of the AMIP simulations include the greater warming over western North America and slight cooling over eastern and southern regions of the United States. The total 1951 to 2006 change in observed North American annual surface temperatures of +0.90°C (about 1.6°F) compares well to the AMIP simulated warming of +0.59°C (almost 1.1°F).

A strong agreement exists between the AMIP and CMIP simulated North American surface temperature trend patterns and their time evolutions during 1951 to 2006. This comparison of the CMIP and AMIP simulations indicates that a substantial fraction of the area-averaged anthropogenic warming over North America has *likely* occurred as a consequence of sea surface temperature forcing. However, the physical processes by which the oceans have led to North American warming is not currently known.

An important attribution challenge is determining which aspects of regional SST variability during 1951 to 2006 have been important in contributing to the signals shown in Figure 3.3. Idealized studies linking regional SST anomalies to atmospheric variability have been conducted (Hoerling *et al.*, 2001; Robertson *et al.*, 2003; Barsugli *et al.*, 2002; Kushnir *et al.*, 2002); however, a comprehensive suite of model simulations to address variability in North American surface temperatures during 1951 to 2006 has not yet been undertaken. Whereas the North American sensitivity to SST forcing from the ENSO region is well understood, the effect of the progressive tropical-wide SST warming, a condition that has been the major driver of globally averaged SST behavior during the last half century, is less well known (Figure 3.5). A further question is the effect that recent decadal warming of the North Pacific and North Atlantic Oceans have had on North American climate, either in explaining the spatial variations in North American temperature trends or as a factor in the accelerated pace of North American warming since 1970. Although the desired simulation suite have yet to be conducted, some attribution evidence for regional SST effects can be learned empirically from the reanalysis data itself, which are capable of describing changes in tropospheric circulation patterns, elements of which are known to have regional SST sources. This will be the subject of further discussion in Section 3.3, where observed changes in PNA and NAO circulation patterns since 1950 are described and their role in North American climate trends is assessed.

North American precipitation exhibits considerably greater variability in both space and time compared with temperature.

3.2.2.2.3 Analysis of Annual Average Rainfall Variability Over North America

North American precipitation exhibits considerably greater variability in both space and time compared with temperature. The annual cycle of precipitation varies greatly across the continent, with maximum winter amounts along western North America, maximum summertime amounts over Mexico and Central America, and comparatively little seasonality over eastern North America. Therefore, it is not surprising that the 1951 to 2006 trends in annual precipitation are mainly regional in nature (Figure 3.6, top). Several of these trends are discussed further in Section 3.3.

For area-averaged North America as a whole, there is no coherent trend in observed precipitation since 1951. The time series of annual values has varied within 10 percent of the 56-year

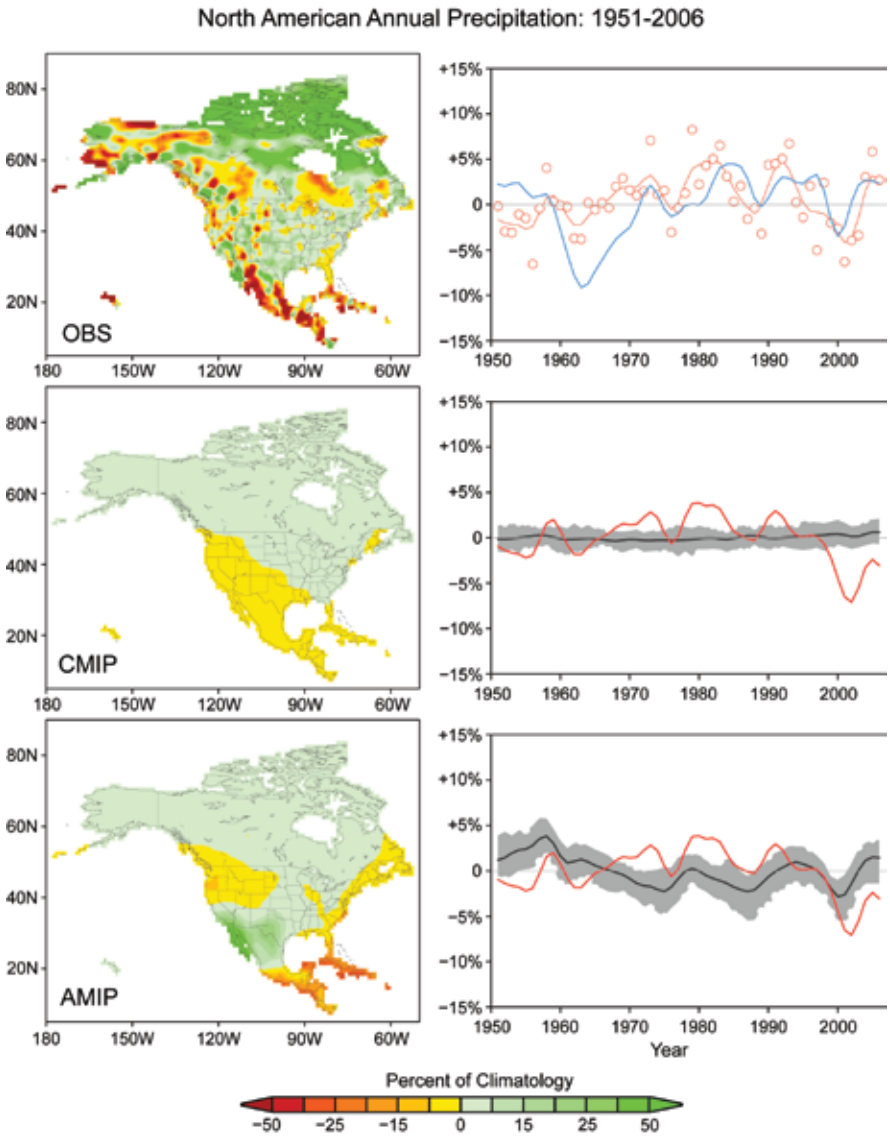

Figure 3.6 The 1951 to 2006 trend in annually averaged North American precipitation from observations (top), CMIP simulations (middle), AMIP simulations (bottom). Maps (left side) show the linear trend in annual precipitations for 1951 to 2006 (units, total 56-year change as percent of the climatological average). Time series (right side) show the annual values from 1951 to 2006 compared as a percentage of the 56-year climatological precipitation average. Curves are smoothed annual values using a five-point Gaussian filter, based on the Global Precipitation Climatology Center observational analysis, and the ensemble mean of climate simulations. The Gaussian filter is a weighted time averaging applied to the raw annual values in order to highlight lower frequency variations. "Five-point" refers to the use of five annual values in the weighting process. Unsmoothed annual observed precipitation is shown by red circles. The blue curve is the NCEP/NCAR reanalysis precipitation over time. For simulations, the gray band contains the 5 to 95 percent occurrence of individual model simulations.

climatological precipitation average, with the most notable feature being the cluster of dry years from the late 1990s to the early 2000s. However, even these annual variations for North American averaged precipitation as a whole are of uncertain physical significance because of the regional focus of precipitation fluctuations and the considerable cancellation between different types of anomalies when averaging across the continent, as is done in Figure 3.6. For instance, above average precipitation due to excess rain in one region can offset below average precipitation due to drought in another region.

Neither externally forced nor SST forced simulations show a significant change in North American-wide precipitation since 1951. In addition, the area-averaged annual fluctuations in the simulations are generally within a few percent of the 56-year climatological average (Figure 3.6, middle and bottom panels). The comparison of the observed and CMIP simulated North America precipitation indicates that the anthropogenic signal is small relative to the observed variability over years and decades. As a note of caution regarding the suitability of the CMIP models for precipitation, the time series of North American precipitation in the individual CMIP simulations show much weaker decadal variability than is observed. Note especially that the recent observed dry anomalies reside well outside the range of outcomes produced by all available CMIP runs, suggesting that the models may underestimate the observed variability, at least for North American annual and area averages.

A small number of detection and attribution studies of average precipitation over land have identified a signal due to volcanic aerosols in low frequency variations of precipitation (Gillett *et al.*, 2004; Lambert *et al.*, 2004). Climate models appear to underestimate both the variation of average precipitation over land compared to observations and the observed precipitation changes in response to volcanic eruptions (Gillett *et al.*, 2004; Lambert *et al.*, 2004). Zhang *et al.* (2007) examined the human influence on precipitation trends over land within latitudinal bands during 1950 to 1999, finding evidence for anthropogenic drying in the subtropics and increased precipitation over sub-polar latitudes,

though observed and greenhouse gas forced simulations disagreed over much of North America.

The time series of North America precipitation from the AMIP simulations shows better agreement with the observations than the CMIP simulations, including marked negative anomalies (*e.g.*, droughts) over the last decade. This suggests that a part of the observed low frequency variations stems from observed variations of global SST. A connection between ENSO-related tropical SST anomalies and rainfall variability over North America has been well documented, particularly for the boreal winter, as mentioned earlier. In addition, the recent years of dryness are consistent with the multi-year occurrence of La Niña (Figure 3.5). The influence of tropical-wide SSTs and droughts in the midlatitudes and North America has also been documented in previous studies (Hoerling and Kumar, 2003; Schubert *et al.*, 2004; Lau *et al.*, 2006; Seager *et al.*, 2005; Herweijer *et al.*, 2006). Such causal links do provide an explanation for the success of AMIP integrations in simulating and explaining some aspects of the observed variability in North American area-averaged precipitation, although it is again important to recognize the limited value of such an area average for describing moisture related climate variations.

3.3 PRESENT UNDERSTANDING OF UNITED STATES SEASONAL AND REGIONAL DIFFERENCES IN TEMPERATURE AND PRECIPITATION TRENDS FROM 1951 TO 2006

3.3.1 Introduction

As noted in the recent IPCC Fourth Assessment Report, identification of human causes for variations or trends in temperature and precipitation at regional and seasonal scales is more difficult than for larger area and annual averages (IPCC, 2007a). The primary reason is that internal climate variability is greater at these scales—averaging over larger space-time scales reduces the magnitude of the internal climate variations (Hegerl *et al.*, 2007). Early idealized studies (Stott and Tett, 1998) indicated that the spatial variations of surface temperature changes due to changes in external forcing, such as greenhouse gas related forcings, would be detectable only at scales of 5000 kilometers (about 3100 miles) or more. However, these signals will be more easily detectable as the magnitude of the expected forced response increases with time. The IPCC Fourth Assessment Report highlights the acceleration of the warming response in recent decades (IPCC, 2007a).

Consistent with increased external forcing in recent decades, several studies (Karoly and Wu, 2005; Knutson *et al.*, 2006; Wu and Karoly, 2007; Hoerling *et al.*, 2007) have shown that the warming trends over the second half of the twentieth century at many individual cells, which are 5° latitude by 5° longitude in area (about 556 by 417 kilometers or 345 by 259 miles), across the globe can now be detected in observations. Further, these are also consistent with the modeled response to anthropogenic climate forcing and cannot be explained by internal variability and response to natural external forcing alone. However, there are a number of regions that do not show significant warming, including the southeast United States, although modeling results have yet to consider a range of other possible forcing factors that may be more important at regional scales, including changes in carbonaceous aerosols (IPCC, 2007a) and changes in land use and land cover (Pielke *et al.*, 2002; McPherson, 2007).

Recent studies have linked some regional and seasonal variations in temperature and precipitation over the United States to variations in sea surface temperature.

What is the current capability to explain spatial variations and seasonal differences in North American climate trends over the past half-century? Can various differences in space and time be accounted for by the climate system's sensitivity to time evolving anthropogenic forcing? To what extent can the influences of natural processes be identified? Recent studies have linked some regional and seasonal variations in temperature and precipitation over the United States to variations in SST (*e.g.*, Livezey *et al.*, 1997; Kumar *et al.*, 2001; Hoerling and Kumar 2002; Schubert *et al.*, 2004; Seager *et al.*, 2005). These published results have either focused on annually averaged or winter-only conditions. This Product will assess both the winter and summer origins change over North America, the contiguous United States, and various sub-regions of the United States.

3.3.2 Temperature Trends

3.3.2.1 North America

The spatial variations in observed North American surface temperature change since 1951 are *unlikely* to be due to anthropogenic forcing alone. The spatial variation of the observed warming over North America is *likely* influenced by observed regional sea surface temperature variations.

The observed annually averaged temperature trends over North America in Figure 3.3 show considerable variation in space, with the largest warming over northern and western North America and least warming over the southeastern United States. The ensemble-averaged model response to anthropogenic and natural forcing since 1951 (CMIP runs in Figure 3.3) shows a more uniform warming pattern, with larger values in higher latitudes and in the interior of the continent. While the spatial correlation of the CMIP simulations with observations for the 1951 to 2006 North American surface temperature trend is 0.79, that agreement is almost entirely due to the agreement in the area-averaged temperature trend. Upon removing the area-averaged warming, a process that highlights the spatial variations, the resulting pattern correlation between trends in CMIP and observations is only 0.13. Thus, the spatial variations in observed North American surface temperature change since 1951 are *unlikely* to be due to anthropogenic forcing alone.

An assessment of AMIP simulations indicates that key features of the spatial variations of annually averaged temperature trends are more consistent with a response to SST variations during 1951 to 2006. The ensemble-averaged model response to observed SST variations (CMIP runs in Figure 3.3) shows a spatial pattern of North American surface temperature trends that agrees well with the observed pattern, with a correlation of 0.87. Upon removing the area-averaged warming, the resulting correlation is still 0.57. This indicates that the spatial variation of the observed warming over North America is *likely* influenced by observed regional SST variations, which is consistent with the previously published results of Robinson *et al.* (2002) and Kunkel *et al.* (2006).

A diagnosis of observed trends in free atmospheric circulation, using the reanalysis data of 500 millibar (mb) pressure heights, provides a physical basis for the observed regionality in North American surface temperature trends. Figure 3.7 illustrates the 1951 to 2006 November to April surface temperature trends together with the superimposed 500 mb height trends. It is during the cold half of the year that many of the spatial features in the annual trend originate, a time during which teleconnection patterns are also best developed and exert their strongest impacts. The reanalysis data captures two prominent features of

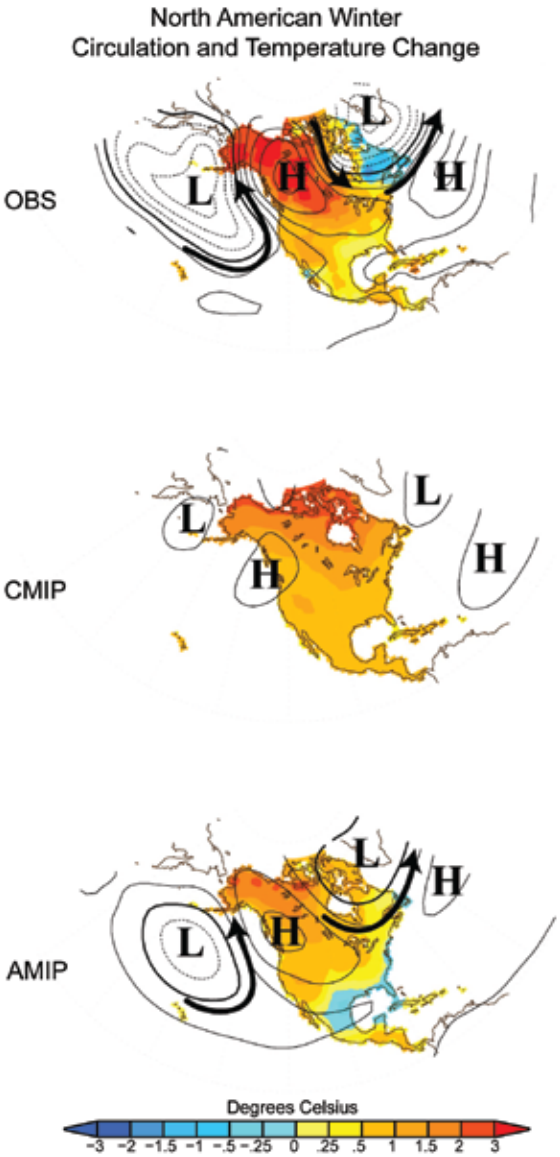

Figure 3.7 The 1951 to 2006 November to April trend of 500 millibars heights (contours, units meters total change over 56 year period, contour interval 10 meters) and North American surface temperature (color shading, units °C total change over 56 year period) for observations (top), CMIP ensemble mean (middle), AMIP ensemble mean (bottom). Anomalous High and Low Pressure regions are highlighted. Arrows indicate the anomalous wind direction, which circulates around the High (Low) Pressure centers in a clockwise (counterclockwise) direction.

circulation change since 1951, one that projects upon the positive phase of the Pacific North American pattern and the other that projects upon the positive phase of the North Atlantic Oscillation pattern. Recalling from Chapter 2 the surface temperature fingerprints attributable to the PNA and NAO, the diagnosis in Figure 3.7 reveals that the pattern of observed surface temperature trend can be understood as a linear combination of two separate physical patterns, consistent with prior published results of Hurrell (1995) and Hurrell (1996).

The historical reanalysis data thus proves invaluable for providing a physically consistent description of the regional structure of North American climate trends. A reason for the inability of the CMIP simulations to replicate key features of the observed spatial variations is revealed by diagnosing their simulated free atmospheric circulation trends, and comparing to the reanalysis data. The CMIP 500 mb height trends (Figure 3.7, middle panel) have little spatial structure, instead being dominated by a nearly uniform increase in heights. Given the strong thermodynamic relation between 500 mb heights and air temperature in the troposphere, the relative uniformity of North American surface warming in the CMIP simulations is consistent with the uniformity in its circulation change (there are additional factors that can influence surface temperature patterns, such as local soil moisture, snow cover and sea ice albedo [amount of short wave radiation reflected] effects on surface energy balances, that may have little influence in 500 mb heights).

In contrast, the ability of the AMIP simulations to produce key features of the observed spatial variations in surface temperature stems from the fact that SST variations during 1951 to 2006 force a trend in atmospheric circulation that projects upon the positive phases of both the PNA and NAO patterns (Figure 3.7, bottom panel). Although the amplitude of the ensemble-averaged AMIP 500 mb height trends is weaker than the observed 500 mb height trends, their spatial agreement is high. It is this spatially varying pattern of the the tropospheric circulation trend since 1951 that permits the reorganization of air mass movements and storm track shifts that is an important factor for explaining key regional details of North American surface climate trends.

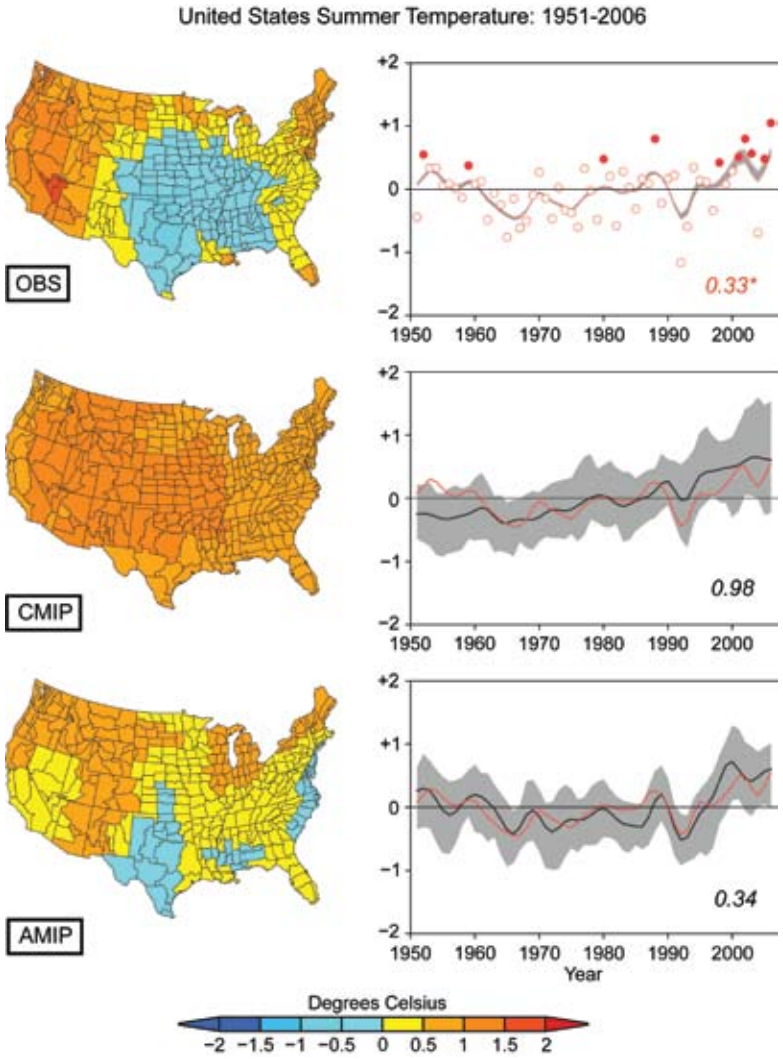

Figure 3.8 Spatial maps of the linear temperature trend (°C total change over 56 year period) in summer (June-July-August) (left side) and time series of the variations over time of United States area-averaged temperatures in summer from observations, CMIP model simulations, and AMIP model simulations. Plotted values are the total 56-year change (°C), with the single asterisk denoting high confidence that an observed change was detected. Gray band in top panel denotes the range of observed temperatures based on five different analyses, gray band in middle panel denotes the 5 to 95 percent range among 41 CMIP model simulations, and gray band in lower panel denotes the 5 to 95 percent range among 33 AMIP model simulations. Curves are smoothed annual values using a five-point Gaussian filter. The Gaussian filter is a weighted time averaging applied to the raw annual values in order to highlight lower frequency variations. "Five-point" refers to the use of five annual values in the weighting process. Unsmoothed observed annual temperature anomalies are shown in open red circles, with warmest ten years shown in closed red circles.

3.3.2.2 Contiguous United States

For the U.S. area-averaged temperature variations, six of the warmest ten summers (Figure 3.8, top) and six of the warmest ten winters (Figure 3.9, top) during 1951 to 2006 occurred in the last decade (1997 to 2006). This recent cluster-

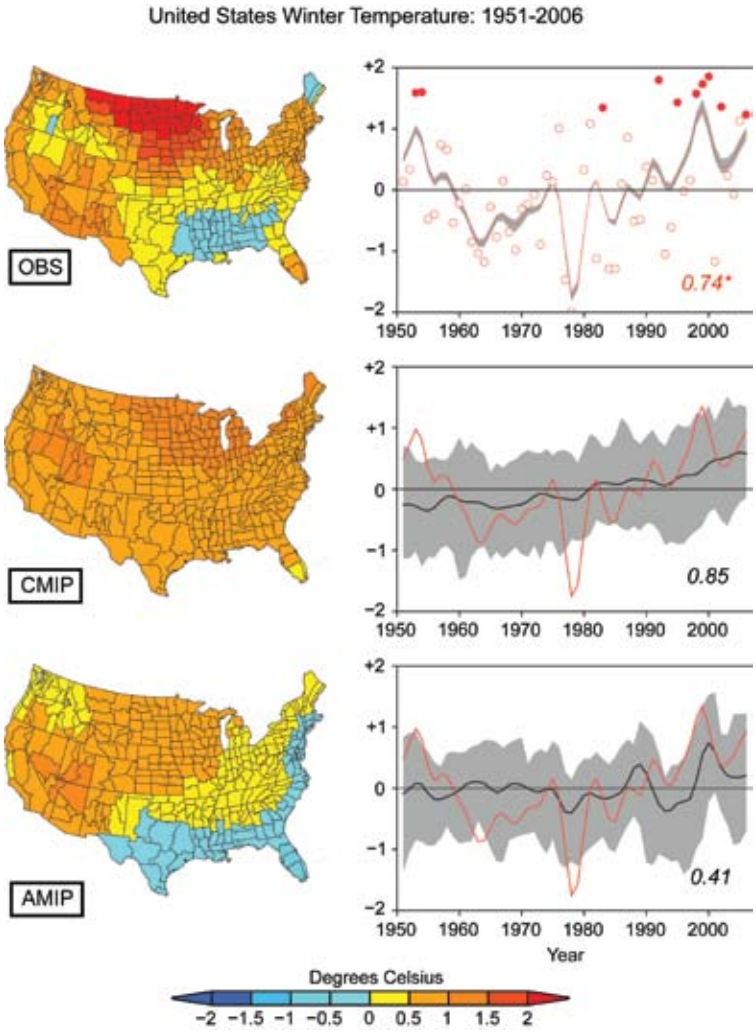

Figure 3.9 Spatial maps of the linear temperature trend (°C total over 56 year period) in winter (December-January-February) (left side) and time series of the variations over time of U.S. area-averaged temperatures in summer from observations, CMIP model simulations, and AMIP model simulations. Plotted values are the total 56-year change (°C), with the double asterisks denoting very high confidence that an observed change was detected. Gray band in top panel denotes the range of observed temperatures based on five different analyses, gray band in middle panel denotes the 5 to 95 percent range among 41 CMIP model simulations, and gray band in lower panel denotes the 5 to 95 percent range among 33 AMIP model simulations. Curves smoothed with five-point Gaussian filter. The Gaussian filter is a weighted time averaging applied to the raw annual values in order to highlight lower frequency variations. "Five-point" refers to the use of five annual values in the weighting process. Unsmoothed observed annual temperature anomalies are shown in open red circles, with warmest ten years shown in closed red circles.

ing of record warm occurrences is consistent with the increasing signal of anthropogenic greenhouse gas warming, as evidenced from the CMIP simulations (Figures 3.8 and 3.9, middle panels) that indicate accelerated warming over the United States during the past decade during both summer and winter.

During summer since 1951, some regions of the United States have observed strong warming while other regions experienced no significant change. The lack of mid-continent warming is a particularly striking feature of the observed trends since 1951, especially compared with the strong warming in the West. This overall pattern of U.S. temperature change is *unlikely* due to anthropogenic forcing alone, an assessment that is supported by several pieces of evidence. First, the spatial variations of the CMIP simulated U.S. temperature trend (Figure 3.8, middle) are not correlated with those observed—the pattern correlation is -0.10 (low and negative correlation) when removing the area-averaged warming. The ensemble CMIP area-averaged summer warming trend of +0.99°C (+1.78°F) is also three times higher than the observed area-averaged warming of +0.33°C (+0.59°F). In other words, there has been much less summertime warming observed for the United States as a whole than expected, based on changes in the external forcing. There is reason to believe, as discussed further below, that internal variations have been masking the anthropogenic greenhouse gas warming signal in summer to date, although the possibility that the simulated signal is too strong cannot be entirely ruled out.

Second, the spatial variations of the AMIP simulations for the U.S. temperature trend (Figure 3.8, bottom) are positively correlated with the observed observations, with a pattern correlation of +0.43 when the area-averaged warming is removed. The cooling of the southern Plains in the AMIP simulations agrees particularly well with observations. The reduced ensemble AMIP area-averaged U.S. summer warming trend of only +0.34°C (+0.61°F) is similar to observations. It thus appears that regional SST variability has played an important role in U.S. summer temperature trends since 1951. The nature of these important SST variations remains unknown. The extent to which they are due to internal coupled system variations and the contribution from anthropogenic forcing are among the vital questions awaiting future attribution research.

During winter, the pattern of observed surface temperature trends (Figure 3.9, top) consists of strong and significant warming over the western

and northern United States, and insignificant change along the Gulf Coast in the South. Both CMIP and AMIP simulations produce key features of the U.S. temperature trend pattern (spatial correlations of 0.70 and 0.57, respectively, upon removing the U.S. area-averaged warming trend), although the cooling along the Gulf Coast appears inconsistent with external forcing, but consistent with SST forcing. The observed U.S. winter warming trend of +0.75°C (1.35°F) has been stronger than that occurring in summer, and compares to an area-averaged warming of +0.85°C (+1.53°F) in the ensemble of CMIP and +0.41°C (+0.74°F) in the ensemble of AMIP simulations.

It is worth noting that the United States also experienced warm conditions during the mid-twentieth century—the early years of available reanalyses (see also Box 3.3 for discussion of the warmth in the United States in the early twentieth century). This is an indication as to how sensitive trends are to the beginning and ending years selected for diagnosis, thus requiring that the trend analysis be accompanied by an assessment of the full evolution over time during 1951 to 2006.

Regarding confidence levels for the observed U.S. temperature trends for 1951 to 2006, a non-parametric test has been applied that estimates the probability distribution of 56-year trends attributable to natural variability alone (see Appendix B for methodological details). As in Section 3.2, this involves diagnosis of 56-year trends from the suite of "naturally forced" CMIP runs, from which a sample of 76 such trends were generated for the contiguous United States for winter and summer seasons. The observed area-averaged U.S. summer trend of +0.33°C (+0.59°F) is found to exceed the 80 percent level of trend occurrences in those natural forced runs, indicating a *high* level of confidence that warming has been detected. For winter, the observed trend of +0.75°C (+1.35°F) is found to exceed the 95 percent level of trends in the natural forced runs indicating a *very high* level of confidence. These diagnoses support this assessment that a warming of U.S. area-averaged temperatures during 1951 to 2006 has *likely* been detected for summer and *very likely* been detected for winter.

A warming of U.S. area-averaged temperatures during 1951 to 2006 has *likely* been detected for summer and *very likely* been detected for winter.

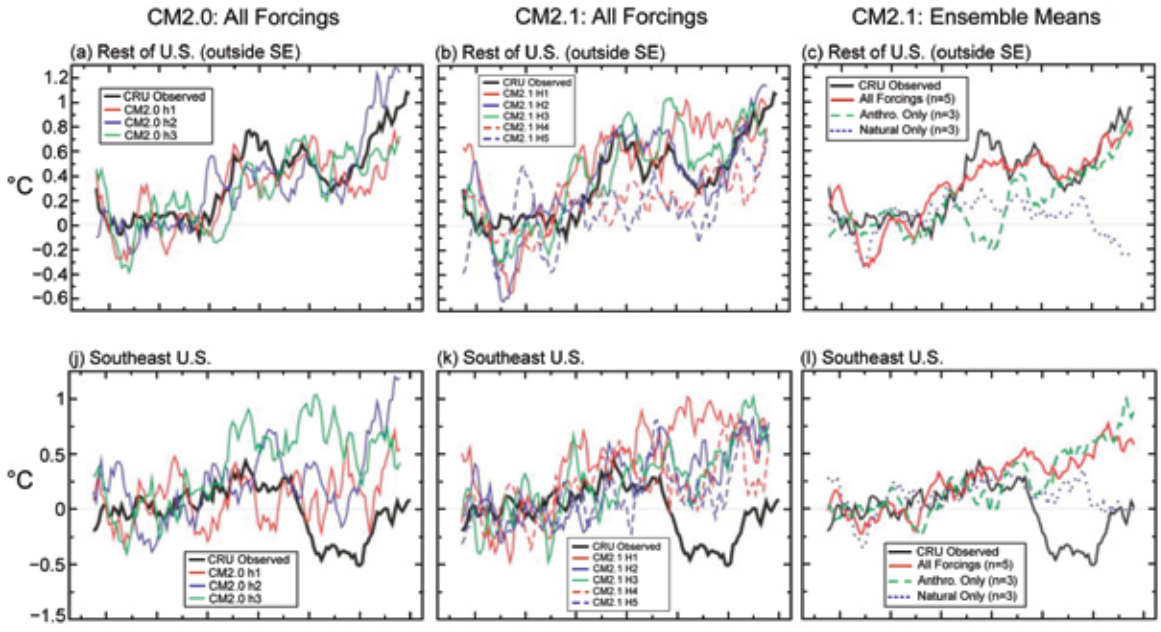

Figure 3.10 Ten-year running-mean area-averaged time series of surface temperature anomalies (°C) relative to 1881 to 1920 for observations and models for various regions: (a) through (c) rest of the contiguous United States, and (j) through (l) U.S. Southeast. The left column and middle columns are based on all-forcing historical runs 1871 to 2000 and observations 1871 to 2004 for GFDL coupled climate model CM2.0 (n=3) and CM2.1 (n=5), respectively. The right column is based on observed and model data through 2000, with ±2 standard error ranges (shading) obtained by sampling several model runs according to observed missing data. The red, blue, and green curves in the right-hand-column diagrams are ensemble mean results for the CM2.1 all-forcing (n=5), natural-only (n=3), and anthropogenic-only (n=3) forcing historical runs. Model data were masked according to observed data coverage. From Knutson *et al.* (2006).

Urbanization, land clearing, deforestation, and reforestation are likely to have contributed to some of the spatial patterns of warming over the United States.

The causes of the reduced warming in the U.S. Southeast compared to the remainder of the country, seen during both winter and summer seasons, have been considered in several studies. Knutson *et al.* (2006) contrasted the area-averaged temperature variations for the Southeast with variations for the remainder of the United States (as shown in Figure 3.10) for both observations and model simulations with the GFDL CM2 coupled model. While the observed and simulated warming due to anthropogenic forcing agrees well for the remainder of the United States, the observed cooling was outside the range of temperature variations that occurred among the small number of individual model simulations performed. For a larger ensemble size, such as provided by the whole CMIP multi-model ensemble as considered by Kunkel *et al.* (2006), the cooling in the Southeast is within the range of model simulated temperature variations but would have to be associated with a very large case of natural cooling superimposed on anthropogenic forced larger scale warming. Robinson *et al.* (2002) and Kunkel *et al.* (2006) have shown that this regional cooling in the central and southeastern United States is associated with the model response to observed SST variations, particularly in the tropical Pacific and North Atlantic oceans, and is consistent with the additional assessment of AMIP simulations presented in this Section.

For the cold half of the year in particular, the Southeast cooling is also consistent with the trends in teleconnection patterns that were diagnosed from the reanalysis data.

Other studies have argued that land use and land cover changes are additional possible factors for explaining the observed spatial variations of warming over the United States since 1951. The marked increase of irrigation in the Central Valley of California and the northern Great Plains is likely to have lead to an increase (warming) in minimum temperatures and a reduced increase (lesser warming) in maximum temperatures in summer (Christy *et al.*, 2006;

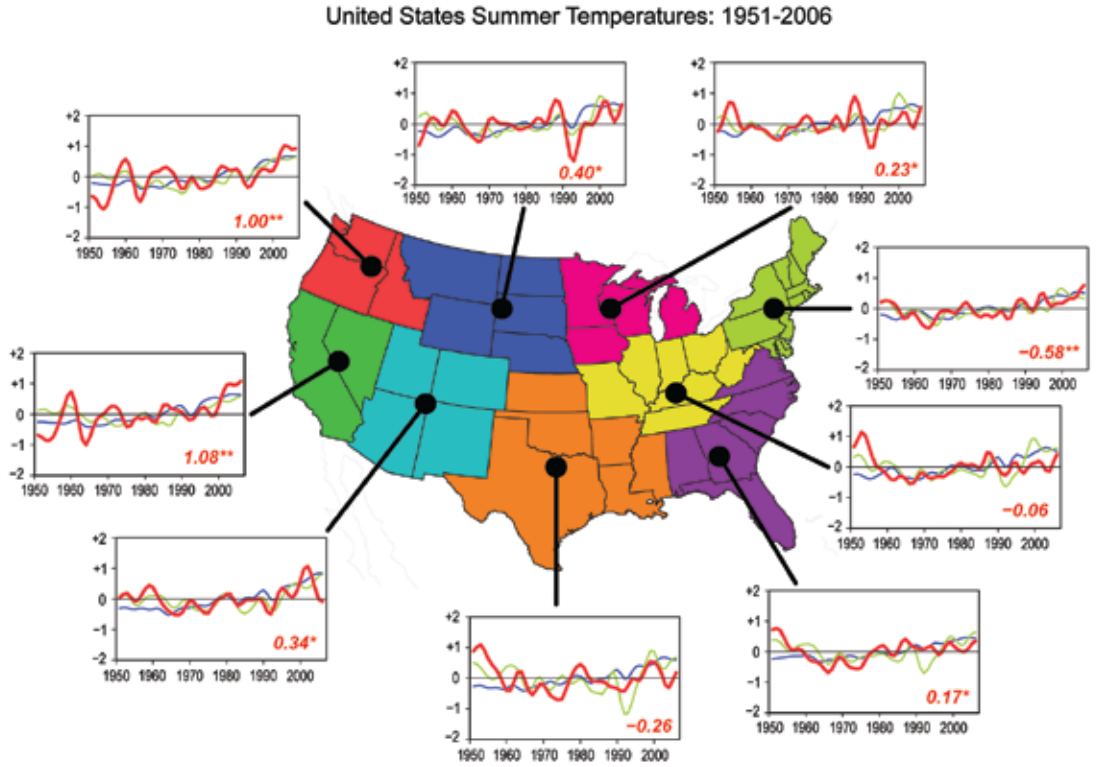

Figure 3.11 Regional U.S. surface temperature changes in summer (June-July-August) from 1951 to 2006. The observations are shown in bold red, ensemble-averaged CMIP in blue, and ensemble-averaged AMIP in green. A five-point Gaussian filter has been applied to the time series to emphasize multi-annual scale time variations. The Gaussian filter is a weighted time averaging applied to the raw annual values in order to highlight lower frequency variations. "Five-point" refers to the use of five annual values in the weighting process. Plotted values in each graph indicate the total 1951 to 2006 temperature change averaged for the sub-region. Double (single) asterisks denote regions where confidence of having detected a change is very high (high).

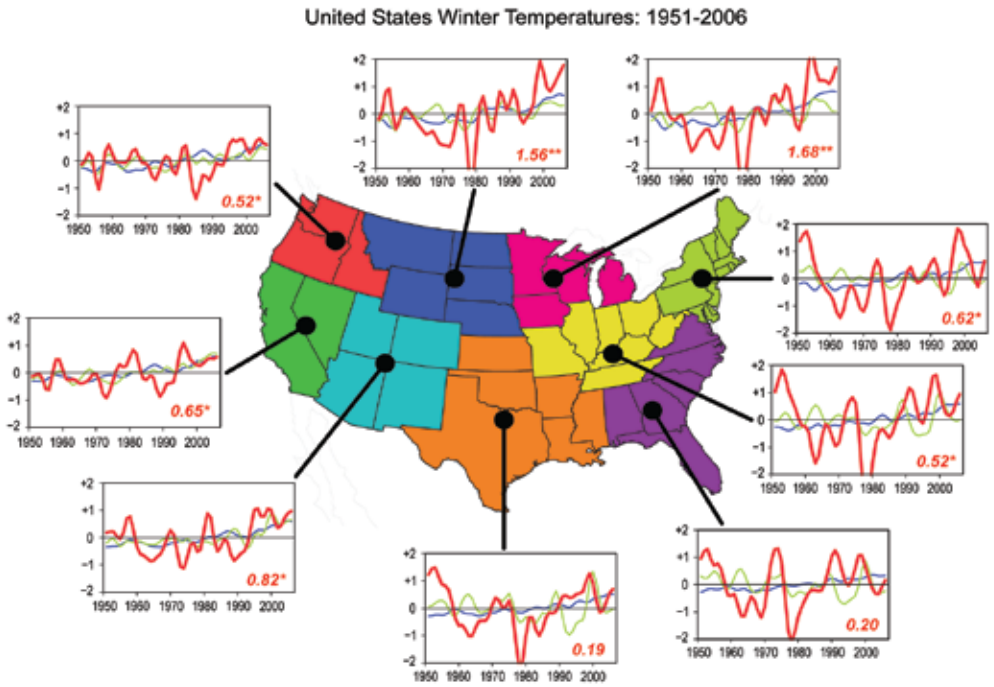

Figure 3.12 Regional U.S. surface temperature changes in winter (December-January-February) from 1951 to 2001. The observations are shown in bold red, ensemble-averaged CMIP in blue, and ensemble-averaged AMIP in green. A five-point Gaussian filter has been applied to the time series to emphasize multi-annual scale time variations. The Gaussian filter is a weighted time averaging applied to the raw annual values in order to highlight lower frequency variations. "Five-point" refers to the use of five annual values in the weighting process. Plotted values in each graph indicate the total 1951 to 2006 temperature change averaged for the sub-region. Single (double) asterisks denote regions where confidence of having detected a change is high (very high).

Kueppers *et al.*, 2007; Mahmood *et al.*, 2006). Urbanization, land clearing, deforestation, and reforestation are likely to have contributed to some of the spatial patterns of warming over the United States, though a quantification of these factors is lacking (Hale *et al.*, 2006; Kalnay and Cai, 2003; Trenberth, 2004; Vose *et al.*, 2004; Kalnay *et al.*, 2006).

As a further assessment of the spatial structure of temperature variations, the summer and winter surface temperature changes from 1951 to 2006 for nine U.S. subregions are shown in Figure 3.11 and 3.12, respectively. The observed temperature change is shown by the red bold curve, and the CMIP and AMIP ensemble-averaged temperature changes are given by blue and green curves, respectively. No attribution of recent climate variations and trends at these scales has been published, aside from the aforementioned Knutson *et al.* (2006) and Kunkel *et al.* (2006) studies that examined conditions over the U.S. Southeast. For decision making at these regional scales, as well as smaller local scales, a systematic explanation of such climate conditions is needed. In this Product, several salient features of the observed and simulated changes are discussed; however, a complete synthesis has yet to be undertaken. For each region of the United States, the total 1951 to 2006 observed surface temperature change and its significance is plotted beneath the time series. Single asterisks denote high confidence and double asterisks denote very high confidence that a change has been detected using the methods described above.

During summer, there is *very high* confidence that warming has been observed over Pacific Northwest and Southwest regions. For these regions, the net warming since 1951 has been about +0.9°C (+1.6°F).

During summer (Figure 3.11), there is *very high* confidence that warming has been observed over Pacific Northwest and Southwest regions. For these regions, the net warming since 1951 has been about +0.9°C (+1.6°F), exceeding the 95 percent level of trends in the natural forced runs at these regional levels. *High* confidence of a detected warming also exists for the Northeast, where the observed 56-year change is not as large, but occurs in a region of reduced variability, thereby increasing detectability of a change. These three warming regions also exhibit the best temporal agreement with the warming simulated in the CMIP models. In addition, the comparatively weaker observed

summertime trends during 1951 to 2006 in the interior West, the southern Great Plains, the Ohio Valley, and the Southeast may be influenced by the very warm conditions at the beginning of the reanalysis record, a period of widespread drought in those regions of the country.

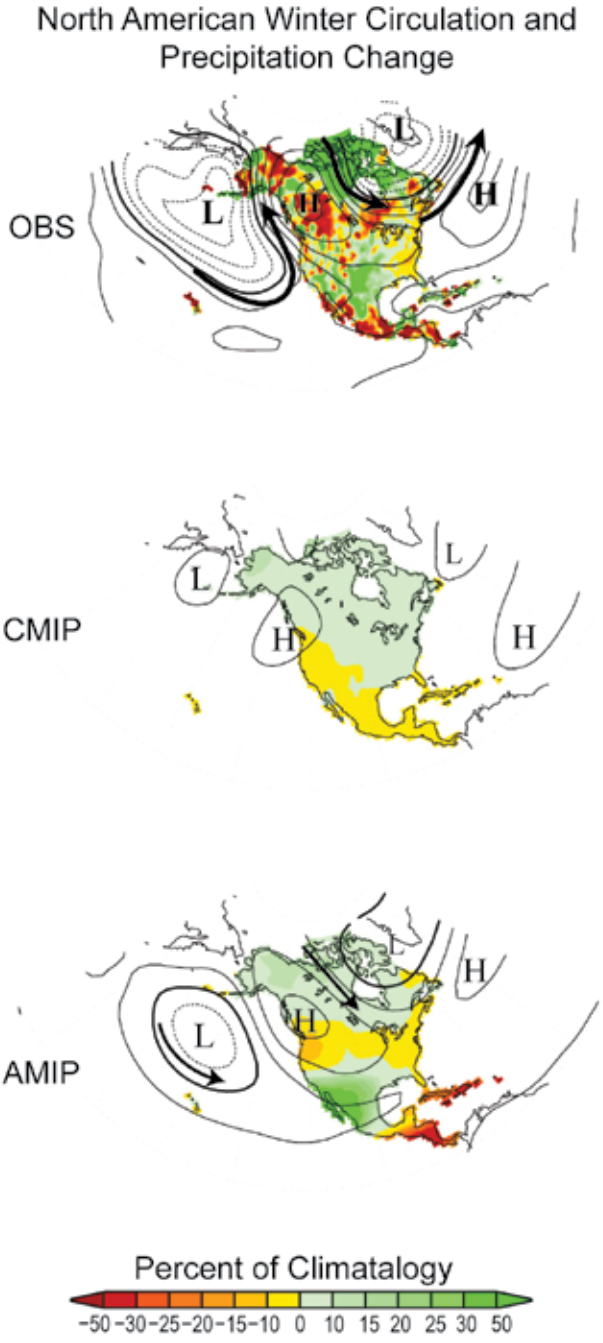

Figure 3.13 The 1951 to 2006 November to April trend of 500 millibar heights (contours, units meters total over 56 year period, contour interval 10 meters) and North American precipitation (color shading, units 56-year change as percent of the 1951 to 2006 climatological average) for observations (top), CMIP ensemble-averaged (middle), AMIP ensemble-averaged (bottom). Anomalous High and Low Pressure regions are highlighted. Arrows indicate the anomalous wind direction, which circulates around the High (Low) Pressure centers in a clockwise (counterclockwise) direction.

During winter (Figure 3.12), there is *very high* confidence that warming has been detected over the northern Great Plains and the Great Lakes region. Confidence is *high* that warming during 1951 to 2006 has been detected in the remaining regions, except along the Gulf Coast in the South, where no detectable change in temperature has occurred. In the northern regions, most of the overall warming of about +1.5°C (+2.7°F) has happened in the last two decades. The CMIP simulations also produce accelerated winter warming over the northern United States in the past 20 years, suggesting that this regional and seasonal feature may have been influenced by anthropogenic forcing.

The 1950s produced some of the warmest winters during the 1951 to 2006 period for several regions of the U.S. The latest decade of warmth in the four southern and eastern United States regions still fails to exceed that earlier decadal warmth. The source for the warm winters in those regions in mid-century is not currently known, and it is unclear whether it is related to a widespread warm period across the Northern Hemisphere during the 1930s and 1940s that was attributed primarily to internal variability (Delworth and Knutson, 2000). The fact that neither CMIP nor AMIP ensemble-averaged responses produce 1950s warmth supports an interpretation that this warmth was likely unrelated to external or the SST forcing.

3.3.3 Precipitation Trends

3.3.3.1 North America

The observed annual North American precipitation trends during 1951 to 2006 in Figure 3.6 are dominated by regional scale features. The prominent identifiable features of change are the annual drying of Mexico and the greater Caribbean region, and the increase over northern Canada. However, due to the strong and differing seasonal cycles of precipitation across the continent, a diagnosis of the annually averaged trends is of limited value. Therefore, this Section focuses further discussion on the seasonal and regional analyses.

The cold-season (November to April) North American observed precipitation change is shown in Figure 3.13 (top), with superimposed contours of the tropospheric circulation change (identical to Figure 3.7). The reanalysis data of circulation change provides physical insights on the origins of the observed regional precipitation change. The band of drying that extends from British Columbia across much of southern Canada and part of the northern United States corresponds to upper level high pressure from which one can infer reduced storminess. In contrast, increased precipitation across the southern United States and northern Mexico in winter is consistent with the deeper southeastward shifted Aleutian low, a semi-permanent low pressure system situated over the Aleutian Islands in winter, that is conducive for increased winter storminess across the southern region of the United States. Further south, drying again appears across southern Mexico and Central America. This regional pattern is unrelated to external forcing alone, as revealed by the lack of spatial agreement with the CMIP trend pattern (middle panel), and the lack of a wavy tropospheric circulation response in the CMIP simulations. However, many key features of the observed regional precipitation change are consistent with the forced response to global SST variations during 1951 to 2006, as is evident from the AMIP trend pattern (bottom). In particular, the AMIP simulations generate the zonal band of enhanced high latitude precipitation, the band of reduced precipitation centered along 45°N, wetness in the southern United States and northern Mexico, and dryness over Central America. These appear to be consistent with the SST forced change in tropospheric circulation. Thus, in future attribution research it is important to determine the responsible regional SST variations, and to assess the origin of the SSTs anomalies themselves.

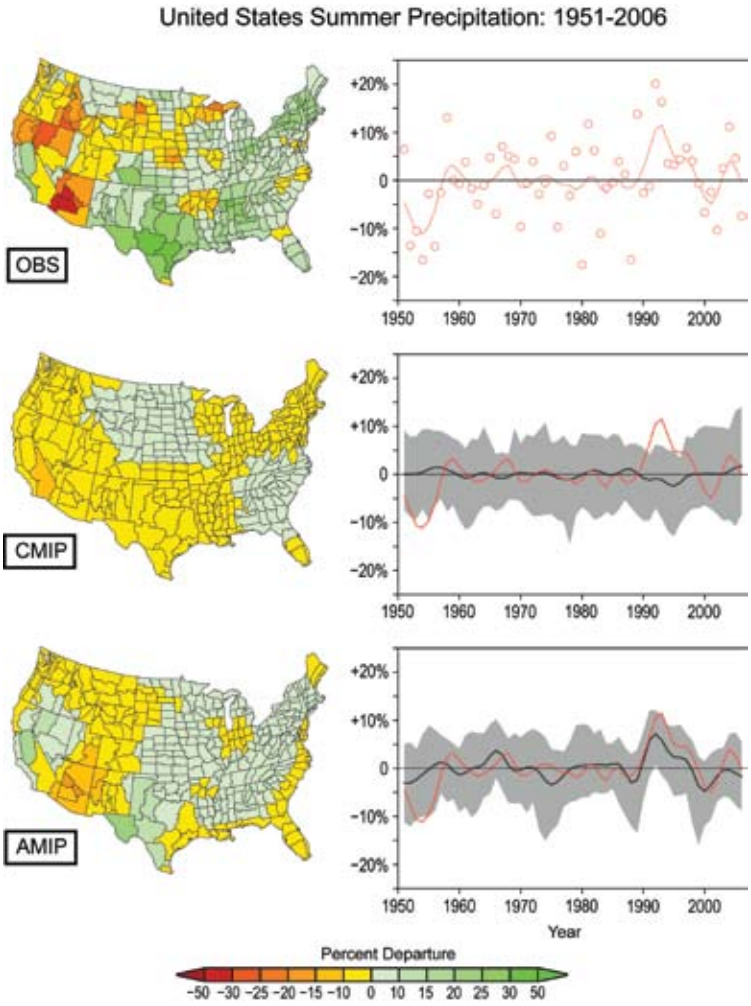

Figure 3.14 Spatial maps of the linear trend in precipitation (percent change of seasonally averaged 1951 to 2006 climatology) in summer (June-July-August) (left side) and the variations over time of U.S. area-averaged precipitation in summer from observations, CMIP model simulations, and AMIP model simulations. Gray band in middle panel denotes the 5 to 95 percent range among 41 CMIP model simulations, and gray band in lower panel denotes the 5 to 95 percent range among 33 AMIP model simulations. Curves smoothed using a five-point Gaussian filter. The Gaussian filter is a weighted time averaging applied to the raw annual values in order to highlight lower frequency variations. "Five-point" refers to the use of five annual values in the weighting process. Unsmoothed observed annual precipitation anomalies are shown in open red circles.

3.3.3.2 Contiguous United States

The observed seasonally-averaged precipitation trends over the period 1951 to 2006 are compared with the ensemble-averaged responses of the CMIP and AMIP simulations for summer in Figure 3.14 and for winter in Figure 3.15. In general, during all seasons there are smaller scale spatial variations of the observed precipitation trends across the United States than for the temperature trends, and larger interannual and decadal variability. These factors undermine the detectability of any physical change in precipitation since 1951.

During summer (Figure 3.14), there is a general pattern of observed rainfall reductions in the U.S. West and Southwest and increases in the East. There is some indication of similar patterns in the CMIP and AMIP simulations, however, the amplitudes are so weak that the ensemble model anomalies are themselves unlikely to be significant. The time series of U.S. summer rainfall is most striking for a recent

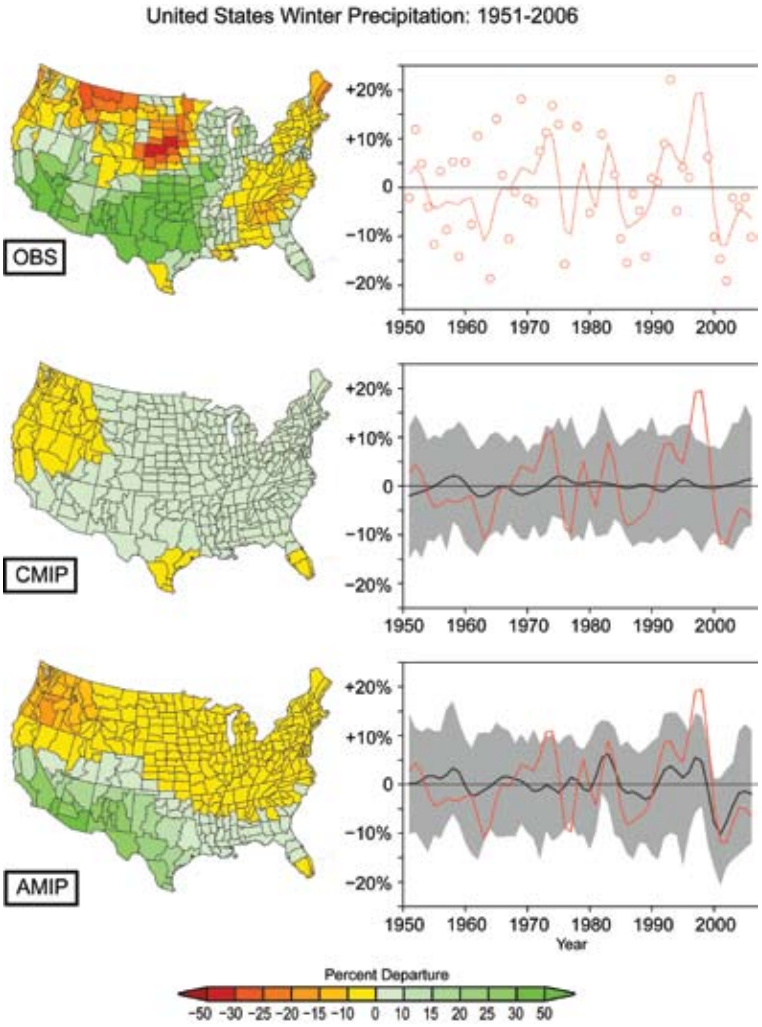

Figure 3.15 Spatial maps of the linear trend in precipitation (percent change of seasonal climatology) in winter (December-January-February) (left side) and the variations over time of U.S. area-averaged precipitation in winter from observations, CMIP model simulations, and AMIP model simulations. Gray band in middle panel denotes the 5 to 95 percent range among 41 CMIP model simulations, and gray band in lower panel denotes the 5 to 95 percent range among 33 AMIP model simulations. Curves smoothed using a five-point Gaussian filter. The Gaussian filter is a weighted time averaging applied to the raw annual values in order to highlight lower frequency variations. "Five-point" refers to the use of five annual values in the weighting process. Unsmoothed observed annual precipitation anomalies are shown in open red circles.

fluctuation between wet conditions in the 1990s, followed by dry conditions in the late 1990s and early 2000s. This prominent variation is well explained by the region's summertime response to SST variations, as seen by the remarkable correspondence of observations with the time evolving AMIP rainfall (lower panel). For the 56-year period as a whole, the temporal correlation of AMIP simulated and observed summer U.S. average rainfall is +0.64.

During winter (Figure 3.15), there is little agreement between the observed and CMIP modeled spatial patterns of trends, though considerably better agreement exists with the AMIP modeled spatial pattern. Again, the ensemble-averaged CMIP model simulations shows no significant long term trends during 1951 to 2006, and they also exhibit weak variability (middle), suggesting that changes in external forcing have had no appreciable influence on area-averaged precipitation in the United States. This is consistent with the published results of Zhang *et al.* (2007) who find disagreement between observed and CMIP simulated trends over the United States. In contrast, several key decadal variations are captured by the ensemble mean AMIP simulations including again the swing from wet 1990s to dry late 1990s early 2000 conditions. For the 56-year period as a whole, the temporal correlation of AMIP simulated and observed winter U.S. average rainfall is +0.59.

For the nine separate U.S. regions, Figures 3.16 and 3.17 illustrate the variations over time of observed, ensemble CMIP, and ensemble AMIP precipitation for summer and winter seasons, respectively. These highlight the strong temporal swings in observed regional precipitation between wet and dry periods, such that no single region has a detectable change in precipitation during 1951 to 2006. These observed fluctuations are nonetheless of great societal relevance, being associated with floods and droughts having catastrophic local impacts. Yet, comparing to CMIP simulations indicates that it is *exceptionally unlikely* that these events are related to external forcing. There is some indication from the AMIP simulations that their occurrence is somewhat determined by SST events, especially in the South and West, during winter presumably related to the ENSO cycle.

Other statistical properties of rainfall, including extremes in daily amounts and the fraction of annual rainfall due to individual wet days have exhibited a detectable change over the United States in recent decades, and such changes have been attributed to anthropogenic forcing in the companion CCSP SAP 3.3 Product (CCSP, 2008).

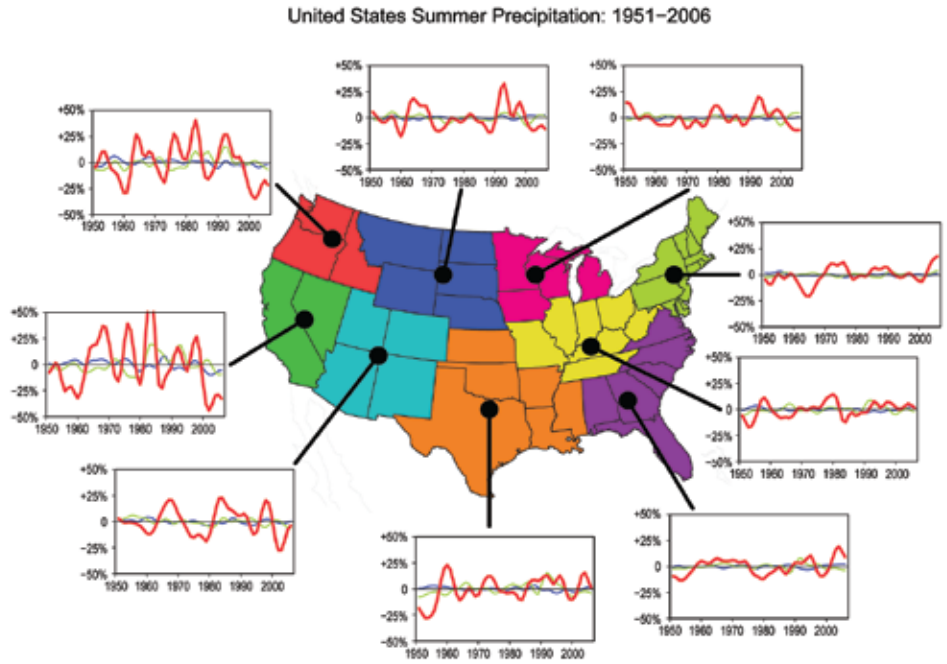

Figure 3.16 The 1951 to 2006 regional U.S. precipitation changes over time in summer (June-July-August). The observations are shown in bold red, ensemble-averaged CMIP in blue, and ensemble-averaged AMIP in green. A five-point Gaussian filter has been applied to the time series to emphasize multi-annual scale time variations. The Gaussian filter is a weighted time averaging applied to the raw annual values in order to highlight lower frequency variations. "Five-point" refers to the use of five annual values in the weighting process.

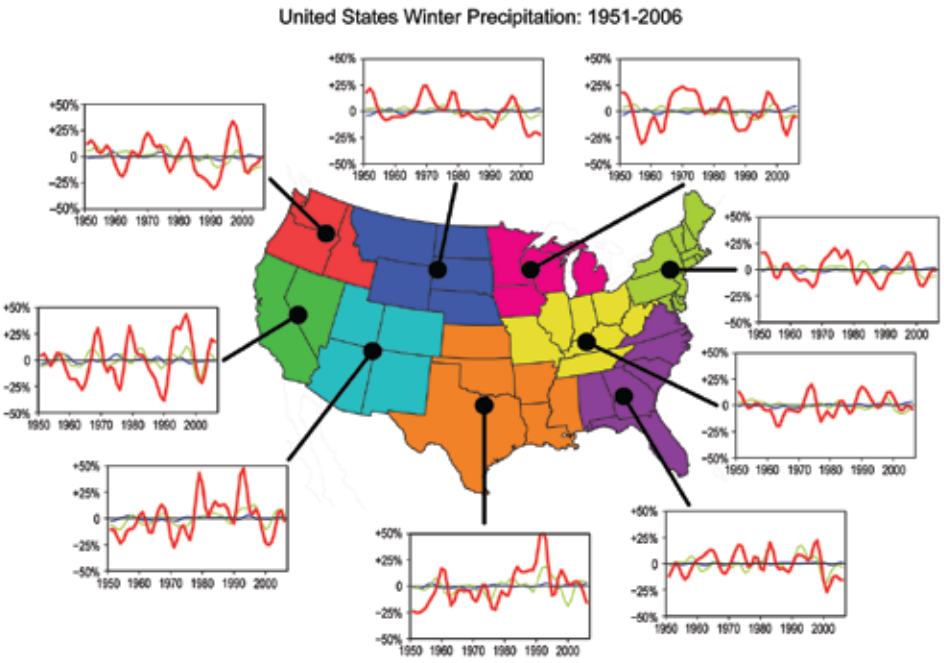

Figure 3.17 The 1951 to 2006 regional U.S. precipitation changes over time in winter (December-January-February). The observations are shown in bold red, ensemble-averaged CMIP in blue, and ensemble-averaged AMIP in green. A five-point Gaussian filter has been applied to the time series to emphasize multi-annual scale time variations. The Gaussian filter is a weighted time averaging applied to the raw annual values in order to highlight lower frequency variations. "Five-point" refers to the use of five annual values in the weighting process.

3.4 NATURE AND CAUSE OF APPARENT RAPID CLIMATE SHIFTS FROM 1951 TO 2006

3.4.1 Introduction

Rapid climate shifts are of scientific interest and of public concern because of the expectation that such occurrences may be particularly effective in exposing the vulnerabilities of societies and ecosystems (Smith *et al.*, 2001). Such abrupt shifts are typically distinguished from the gradual pace of climate change associated, for instance, with anthropogenic greenhouse gas forcing. However, through non-linear feedbacks, gradual forcing could also trigger rapid shifts in some parts of the climate system, a frequently cited example being a possible collapse of the global ocean's principal conveyor of heat between the tropics and high latitudes known as the thermohaline circulation (Clarke *et al.*, 2002).

A rapid climate shift is one occurring so fast that societies and ecosystems have difficulty adapting to it.

By their very nature, abrupt shifts are unexpected events—climate surprises—and thus offer particular challenges to policy makers in planning for their impacts. A retrospective assessment of such "rare" events may offer insights on mitigation strategies that are consistent with the severity of impacts related to rapid climate shifts. Such an assessment would also consider impacts of abrupt climate shifts on societies and ecosystems and would also prepare decision makers to anticipate consequences of gradual changes in climate, insofar as they may be no less severe than those related to rapid climate shifts.

3.4.2 Defining Rapid Climate Shifts

A precise definition for a climate shift that is either "rapid" or "abrupt" does not exist because there is limited knowledge about the full sensitivity of the climate system. For instance, due to nonlinearity, changes in external forcing may not lead to a proportionate climate response. It is conceivable that a *gradual* change in external forcing could yield an abrupt response when applied near a tipping point (the point at which a slow gradual change becomes irreversible and then proceeds at a faster rate of change) of sensitivity in the climate system, whereas an *abrupt* change in forcing may not lead to any abrupt response when it is applied far from the system's tipping point. To date, little is known about the threshold tipping points of the climate system (Alley *et al.*, 2003).

In its broadest sense, a "rapid" shift is a transition between two climatic states that individually have much longer duration than the transition period itself. From an impacts viewpoint, a rapid climate shift is one occurring so fast that societies and ecosystems have difficulty adapting to it.

3.4.3 Mechanisms for Rapid Climate Shifts

The National Research Council (NRC, 2002) has undertaken a comprehensive assessment of rapid climate change, summarizing evidence of such changes occurring before the instrumental and reanalysis records, and understanding abrupt changes in the modern era. The NRC (2002) report on abrupt climate change draws attention to evidence for severe swings in climate proxies of temperature (so-called paleoreconstructions) during both the last ice age and the subsequent interglacial period known as the Holocene. Ice core data indicate that abrupt shifts in climate have often occurred during Earth's climate history, indicating that gradual and smooth movements do not always characterize climate variations. Identification of such shifts is usually empirical, based upon expert assessment of long time series of the relevant climate records, and in this regard, their recognition is retrospective. Against this background of abundant evidence for the magnitude of rapid climate shifts, there is a lack of information about the mechanisms that can lead to climate shifts and of the processes by which climate is maintained in various altered states (Broecker, 2003). Understanding the causes of such shifts is a prerequisite to any early warning system that is, among other purposes, needed for planning the scope and pace of mitigation.

The National Academy report (NRC, 2002) also highlights three possible mechanisms for abrupt change: (1) an abrupt forcing, such as may occur through meteorite impacts or volcanic eruptions; (2) a threshold-like sensitivity of the climate system in which sudden changes can occur even when subjected to gradual changes in forcing; and (3) an unforced behavior of the climate system resulting purely from chaotic internal variations.

3.4.4 Rapid Climate Shifts since 1950

Although changes in external forcing, whether natural or anthropogenic, are not yet directly assimilated in the current generation of reanalysis products, abrupt changes in external forcings can still influence the reanalyses indirectly through their effect on other assimilated variables. Observational analyses of the recent instrumental record give some clues of sudden climate shifts, characterized as those that have had known societal consequences. These are summarized below according to the current understanding of the potential mechanism involved. For several reasons, the sustainability of these apparent shifts is not entirely known. First, since 1950, multi-decadal fluctuations are readily seen in North American temperatures (Figure 3.3) and precipitation (Figure 3.6). Although the post-1950 period is the most accurately observed period of Earth's climate history, the semi-permanency of any change cannot be readily judged from merely 50 years of data. This limited perspective of our brief modern climate record stands in contrast to proxy climate records, within which stable climate was punctuated by abrupt change leading to new climate states lasting centuries to millennia. Second, it is not known whether any recent rapid transitions have involved threshold exceedences in a manner that would forewarn of their permanence.

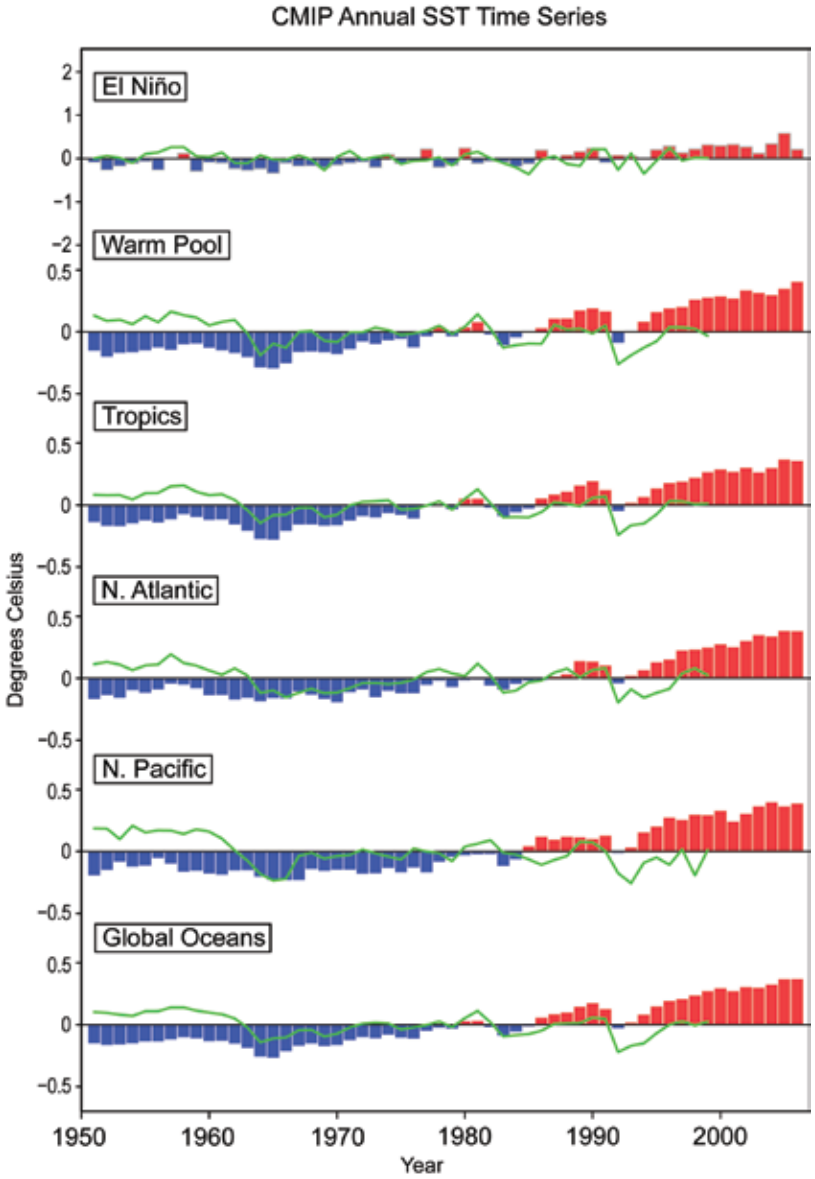

Figure 3.18 CMIP simulated annually-averaged SST changes over time for 1951 to 2006. The oceanic regions used to compute the indices are 5°N to 5°S, 90°W to 150°W for El Niño, 10°S to 10°N, 60°E to 150°E for the warm pool, 30°S to 30°N for the tropics, 30°N to 60°N for the North Atlantic, 30°N to 60°N for the North Pacific, and 40°S to 60°N for the global oceans. Dataset is the ensemble average of 19 CMIP models subjected to the combination of external anthropogenic and natural forcing, and anomalies are calculated relative to each model's 1951 to 2006 reference. Green curve is the surface temperature change based on the ensemble average of four CMIP models forced only by time evolving natural forcing (volcanic and solar).

3.4.4.1 Abrupt Natural External Forcings since 1950

The period of the reanalysis record was a volcanically active one, particularly compared with the first half of the twentieth century. Three major volcanic eruptions included the Agung in 1963, El Chichon in 1982, and Mt. Pinatubo in 1991. Each eruption injected aerosols into the stratosphere (about 10 kilometers, or 6 miles, above the Earth's surface), acting to significantly increase the stratospheric aerosol optical depth that led to an increase in the reflectance of incoming solar radiation (Santer *et al.*, 2006).

Each of these abrupt volcanic forcings has been found to exert a discernable impact on climate conditions. Observed sea surface temperatures cooled in the wake of the eruptions, the detectability of which was largest in oceans having small unforced, internal variability (Santer *et al.*, 2006). Surface-based observational analyses of these and other historical volcanoes indicate that North American surface temperatures tend to experience warming in the winters following strong eruptions, but cooling in the subsequent summer (Kirchner *et al.*, 1999). However, these abrupt forcings have not led to sustained changes in climate conditions, namely because

the residence time for the stratospheric aerosol increases due to volcano eruption is less than a few years (depending on the particle sizes and the geographical location of the volcanic eruption), and the fact that major volcanic events since 1950 have been well separated in time.

The impact of the volcanic events is readily seen in Figure 3.18 (green curve) which plots annual SST changes over time in various ocean basins derived from the ensemble-averaged CMIP simulations forced externally by estimates of the time evolving volcanic and solar forcings (so-called "natural forcing" runs). The SST cooling in the wake of each event is evident. Furthermore, in the comparison with SST evolutions in the fully forced natural and anthropogenic CMIP runs (Figure 3.18, bars), the lull in ocean warming in the early 1980s and early 1990s was likely the result of the volcanic aerosol effects. Similar lulls in warming rates are evident in the observed SSTs at these times (Figure 3.5). They are also evident in the observed and CMIP simulated North American surface temperature changes over time (Figure 3.3). Yet, while having detected the climate system's response to abrupt forcing, and while some model simulations detect decade-long reductions in oceanic heat content following volcanic eruptions (Church *et al.*, 2005), their impacts on surface temperature have been relatively brief and transitory.

Some rapid climate transitions in recent decades appear attributable to chaotic natural fluctuations.

3.4.4.2 Abruptness related to gradual increase of greenhouse gases since 1950

Has the gradual increase in greenhouse gas external forcing triggered threshold-like behavior in climate, and what has been the relevance for North America? There is evidence of abrupt changes of ecosystems in response to anthropogenic forcing that is consistent with tipping point behavior over North America (Adger *et al.*, 2007). Some elements of the physical climate system including sea ice, snow cover, mountainous snowpack, and streamflow have also exhibited rapid change in recent decades (IPCC, 2007a).

There is also some suggestion of abrupt change in ocean surface temperatures. Whereas the overall global radiative forcing due to increasing greenhouse gases has increased steadily since 1950 (IPCC, 2007a), observed sea surface temperature over the warmest regions of the world ocean—the so-called warm pool—experienced a rapid shift to warm conditions in the late 1970s (Figure 3.5). In this region covering the tropical Indian Ocean/West Pacific where surface temperatures can exceed 30°C (86°F), the noise of internal SST variability is weak, increasing the confidence in the detection of change. While there is some temporal correspondence between the rapid 1970s emergent warm pool warming in observations and CMIP simulations (Figure 3.18), further research is required to confirm that a threshold-like response of the ocean surface heat balance to steady anthropogenic forcing occurred.

The matter of the relevance of abrupt oceanic warming for North American climate is even less clear. On one hand, North American surface temperatures also warmed primarily after the 1970s, although not in an abrupt manner. The fact that the AMIP simulations yield a similar behavior suggests some cause-effect link to the oceans. On the other hand, the CMIP simulations generate a steadier rate of North American warming during the reanalysis period, punctuated by brief pauses due to volcanic aerosol-induced cooling events.

3.4.4.3 Abruptness due to unforced chaotic behavior since 1950

Some rapid climate transitions in recent decades appear attributable to chaotic natural fluctuations. One focus of studies has been the consequence of an apparent shift in the character of ENSO events after the 1970s, with more frequent El Niño warming in recent decades (Trenberth and Hoar, 1996).

Abrupt decreases in rainfall occurred over the U.S. Southwest and Mexico in the 1950s and 1960s (Narisma *et al.*, 2007), with a period of enhanced La Niña conditions during that decade being a likely cause (Schubert *et al.*, 2004; Seager *et al.*, 2005). However, this dry period, and the decadal period of the Dust Bowl that preceded it over the Great Plains, did not constitute permanent declines in those regions' rainfall, despite meeting some criteria for detecting abrupt rainfall changes (Narisma *et al.*, 2007). In part, the ocean conditions that

contributed to these droughts did not persist in their cold La Niña state.

An apparent rapid transition of the atmosphere-ocean system over the North Pacific was observed to occur in the period from 1976 to 1977. From an oceanographic perspective, changes in ocean heat content and SSTs that happened suddenly over the Pacific basin north of 30°N were caused by atmospheric circulation anomalies (Miller *et al.*, 1994). These consisted of an unusually strong Aleutian Low that developed in the fall season of 1976, a feature that recurred during many successive winters for the next decade (Trenberth, 1990). These surface features were linked with a persistent positive phase of the PNA teleconnection pattern in the free atmosphere as revealed by reanalysis data. The time series of wintertime Alaskan surface temperatures (Figure 3.19) reveals the mild conditions that suddenly emerged after 1976. This transition in climate was accompanied by significant shifts in marine ecosystems throughout the Pacific Basin (Mantua *et al.*, 1997). It is now evident that this Pacific Basin-North American event, while perhaps meeting some criteria for a rapid transition, was mostly due to a large scale coupled-ocean atmosphere variation over multiple decades (Latif and Barnett, 1996). Thus, it is best viewed as a climate "variation" rather than as an abrupt change in the coupled ocean-atmosphere system (Miller *et al.*, 1994). Such multidecadal variations are readily seen in the observed index of both the North Pacific and the North Atlantic SSTs. However, the Alaskan temperature time series also indicates that there has been no return to cooler surface conditions in recent years. While the pace of anthropogenic warming alone during the last half-century has been more gradual than the rapid warming observed over Alaska, the superposition of an internal decadal fluctuation can lend the appearance of an abrupt warming, as Figure 3.19 indicates occurred over western North America in the mid-1970s. It is plausible that the permanency of the shifted surface warmth is rendered by the progressive increase in the strength of the external anthropogenic signal relative to the amplitude of internal decadal variability.

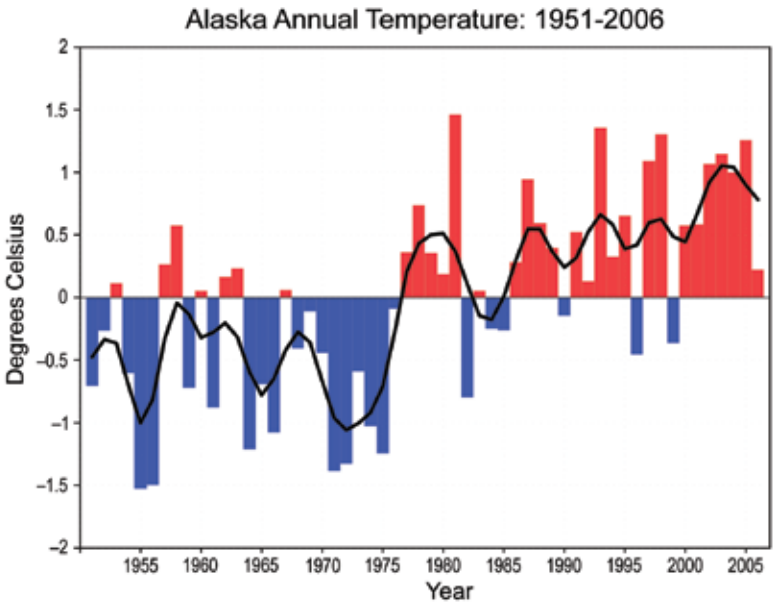

Figure 3.19 Observed Alaska annual surface temperature departures for 1951 to 2006. Anomalies are calculated relative to a 1951 to 2006 reference. Smoothed curve is a five-point Gaussian filter applied to the annual departures to emphasize multi-annual variations. The Gaussian filter is a weighted time averaging applied to the raw annual values in order to highlight lower frequency variations. "Five-point" refers to the use of five annual values in the weighting process.

3.5 UNDERSTANDING OF THE CAUSES FOR NORTH AMERICAN HIGH-IMPACT DROUGHT EVENTS FOR 1951 TO 2006

3.5.1. Introduction

Climate science has made considerable progress in understanding the processes leading to drought, due in large part to the emergence of global observing systems. The analysis of the observational data reveals relationships with large-scale atmospheric circulation patterns, and illustrates linkages with sea surface temperature patterns as far away from North America as the equatorial Pacific and Indian Ocean. Computing capabilities to perform extensive experimentation—only recently available—are permitting first ever quantifications of the sensitivity of North American climate to various forcings, including ocean temperatures and atmospheric chemical composition.

Credible prediction systems are always improved when supported by knowledge of the underlying mechanisms and causes for the phenomenon's variability.

Such progress, together with the recognition that the U.S. economy suffers during severe droughts, has led to the launch of a National Integrated Drought Information System (NIDIS, 2004), whose ultimate purpose is to develop a timely and useful early warning system for drought.

Credible prediction systems are always improved when supported by knowledge of the underlying mechanisms and causes for the phenomenon's variability. In this Section, current understanding of the origins of North American drought is assessed, focusing on events during the period of abundant global observations since about 1950. Assessments of earlier known droughts (such as the Dust Bowl) serve to identify potential cause-effect relationships that may apply to more recent and future North American regional droughts, and this perspective is provided as well (see Box 3.3 for discussion of the Dust Bowl).

The North American continent has experienced numerous periods of drought during the reanalysis period, 1951 to 2006.

3.5.2 Definition of Drought

Many definitions for drought appear in the literature, each reflecting its own unique social and economic context in which drought information is desired. In this Product, the focus is on meteorological drought as opposed to the numerous impacts (and measures) that could be used to characterize drought (*e.g.*, the hydrologic drought, indicated by low river flow and reservoir storage, or the agricultural drought, indicated by low soil moisture and deficient plant yield).

Meteorological drought has been defined as "a period of abnormally dry weather sufficiently prolonged for the lack of water to cause serious hydrologic imbalance in the affected area" (Huschke, 1959). The policy statement of the American Meteorological Society defines meteorological and climatological drought in terms of the magnitude of a precpitation shortfall and the duration of this shortfall event (AMS, 2004).

The Palmer Drought Severity Index (PDSI) (Palmer, 1965) measures the deficit in moisture supply relative to its demand at the Earth's surface, and is used in this Chapter to illustrate some of the major temporal variations of drought witnessed over North America. The Palmer Drought Index is also useful when intercomparing historical droughts over different geographical regions (*e.g.*, Karl, 1983; Diaz, 1983), and it has been found to be a useful proxy of soil moisture and streamflow deficits that relate to the drought impacts having decision-making relevance (*e.g.*, Dai *et al.*, 2004).

3.5.3 Drought Causes

3.5.3.1 Drought Statistics, Mechanisms and Processes

The North American continent has experienced numerous periods of drought during the reanalysis period. Figure 3.20 illustrates the time variability of areal coverage of severe drought since 1951, and on average, 10 percent (14 percent) of the area of the contiguous (western) United States experiences severe drought each year. The average PDSI for the western states during this time period is shown in the bottom panel; while it is very likely dominated by internal variability, the severity of the recent drought compared with others since 1950 is also apparent.

The middle of the twentieth century began with severe drought that covered much of the United

BOX 3.5: Drought Attribution and Use of Reanalysis Data

The indications for drought itself, such as the Palmer Drought Severity Index (PDSI) or precipitation, are not derived from reanalysis data, but from the network of surface observations. The strength of reanalysis data lies in its depiction of the primary variables of the free atmospheric circulation and linking them with the variability in the PDSI. As discussed in Chapter 3, the development and maintenance of atmospheric ridges is the prime ingredient for drought conditions, and reanalysis data is useful for understanding the etymology of such events: their relationship to initial atmospheric conditions, potential downstream and upstream linkages, and the circulation response to soil moisture deficits and SST anomalies. Many drought studies compare model simulations of hypothetical causes to observed atmospheric circulation parameters; reanalysis data can help differentiate among the different possible causes by depicting key physical processes by which drought events evolved.

For final attribution, the drought mechanism must be related to either a specific forcing or internal variability. Reanalysis data, available only since about 1950, is of too short a length to provide a firm indication of internal variability. It also does not indicate (or utilize) direct impact of changing climate forcings, such as increased greenhouse gases or varying solar irradiance. The relationship of atmospheric circulation changes to these forcings must be provided by empirical correlation or, better yet, General Circulation Model (GCM) studies where cause and effect can be directly related.

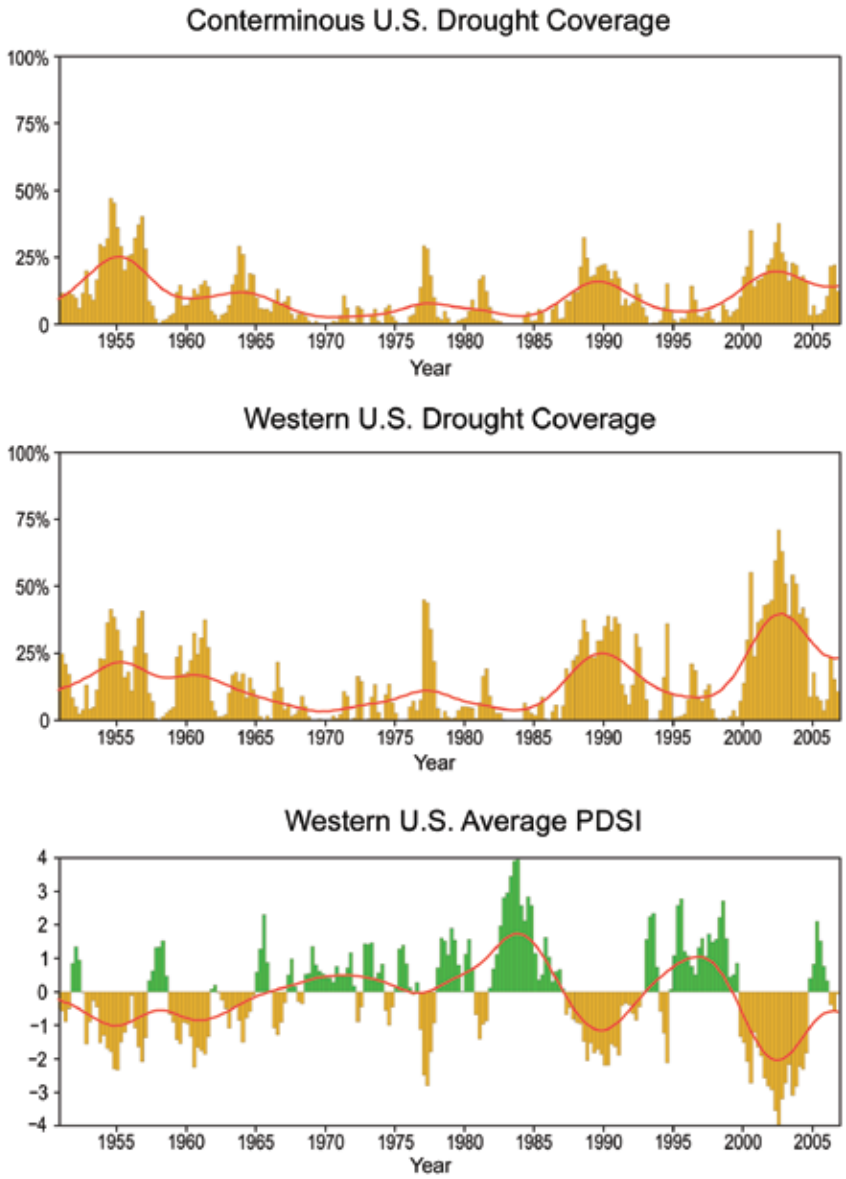

Figure 3.20 Percentage of contiguous United States (top) and western United States (middle) covered by severe or extreme drought, as defined by Palmer Drought Severity Index (PDSI) as less than -3. Time series of the western United States area-averaged PDSI. Positive (Negative) PDSI indicative of above (below) average surface moisture conditions. The western United States consists of the 11 western-most contiguous U.S. states. Red lines depict the time series smoothed using a nine-point Gaussian filter in order to emphasize lower frequency variations. The Gaussian filter is a weighted time averaging applied to the raw annual values. "Five-point" refers to the use of five annual values in the weighting process.

States. Figure 3.21 illustrates the observed surface temperature (top) and precipitation anomalies (bottom) during the early 1950s drought. The superimposed contours are of the 500 mb height from reanalysis data that indicates one of the primary causal mechanisms for drought: high pressure over and upstream that steers moisture-bearing storms away from the drought-affected region.

The northeastern United States had severe drought from about 1962 to 1966, with dry conditions extending southwestward into Texas. The 1970s were relatively free from severe drought, and since 1980 there has been an increased frequency of what the National Climatic Data Center (NCDC) refers to as "billion dollar United States weather disasters", including several major drought events: (1) Summer 1980, central/eastern United States; (2) Summer 1986,

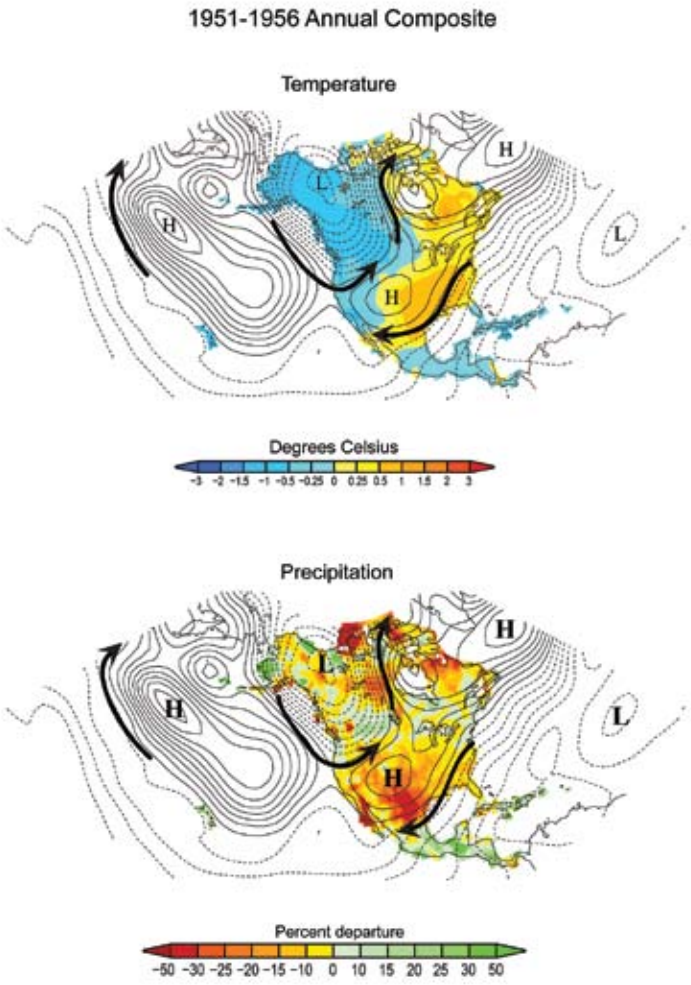

Figure 3.21 Observed climate conditions averaged for 1951 to 1956 during a period of severe U.S. Southwest drought. The 500 millibar height field (contours, units\meters) is from the NCEP/NCAR R1 reanalysis. The shading indicates the five-year average anomaly of the surface temperature (top) and precipitation (bottom). The surface temperature and precipitation are from independent observational datasets. Anomalous High and Low Pressure regions are highlighted. Arrows indicate the anomalous wind direction, which circulates around the High (Low) Pressure centers in a clockwise (counterclockwise) direction.

southeastern United States; (3) Summer 1988, central/eastern United States; (4) Fall 1995 to Summer 1996, U.S. southern plains; (5) Summer 1998, U.S. southern plains; (6) Summer 1999, eastern United States; (7) 2000 to 2002 western United States/U.S. Great Plains; (8) Spring/summer 2006, centered in Great Plains but widespread.

The droughts discussed above cover various parts of the United States, but droughts are most common in the central and southern Great Plains. Shown in Figure 3.22 is the average summer precipitation for the United States (top) and the seasonal standard deviation for the period 1951 to 2006 (bottom). The largest variability occurs along the 95°W meridian, while the lowest variability relative to the average precipitation is in the northeast, a distribution that parallels the occurrence of summertime droughts. This picture is somewhat less representative of droughts in the western United States, a region which receives most of its precipitation during winter.

It is natural to ask whether the plethora of recent severe drought conditions identified by NCDC is associated with human effects, particularly greenhouse gas emissions. Figure 3.20 shows that the United States area covered by recent droughts (lower panel) is similar to that which prevailed in the 1950s, and also similar to conditions before the reanalysis period such as the "Dust Bowl" era of the 1930s (Box 3.3). Paleoreconstructions of drought conditions for the western United States (upper panel) indicate that recent droughts are considerably less severe and protracted than those that have been estimated for time periods in the twelfth and thirteenth centuries from tree ring data (Cook *et al.*, 2004). Hence, from a frequency/area standpoint, droughts in the recent decades are not particularly outstanding. The causes for these droughts need to be better understood in order to better assess human influences on drought.

While drought can have many definitions, all of the episodes discussed relate to a specific weather pattern that resulted in reduced rainfall, generally to amounts less than 50 percent of average precipitation values. The specific weather pattern in question features an amplified broad-scale high pressure area (ridge) in the troposphere over the affected region (Figure 3.21). Sinking air motion associated with a ridge reduces summertime convective rainfall, results in clear skies with abundant sunshine reaching the surface, and provides for a low-level wind flow that generally prevents substantial moisture advection into the region.

The establishment of a stationary wave pattern in the atmosphere is thus essential for generating severe drought. Such stationary, or blocked atmospheric flow patterns can arise due to mechanisms internal to the atmosphere, and the ensuing droughts can be thought of as due to internal atmospheric processes—so-called

unforced variability. However, the longer the anomalous weather conditions persist, the more likely it is to have some stationary forcing acting as a flywheel (*i.e.*, as a source for inertia) to maintain the anomalies.

The droughts discussed above can be distinguished by their duration, with longer lasting events more likely involving forcing of the atmosphere. The atmosphere does not have much heat capacity, and its "memory" of past conditions is relatively short (on the order of a few weeks). Hence, the forcing required to sustain a drought over seasons or years would be expected to lie outside of the atmospheric domain; an obvious possibility with greater heat capacity (and hence a longer "memory") is the ocean. Therefore, most studies have assessed the ability of particular ocean sea surface temperature patterns to generate the atmospheric wave pattern that would result in tropospheric ridges in the observed locations during drought episodes.

Namias (1983) pointed out that the flow pattern responsible for Great Plains droughts, with a ridge over the central United States, also includes other regions of ridging, one in the East Central Pacific and the other in the East Central Atlantic. As described in Chapter 2 and Section 3.1, these teleconnections represent a standing Rossby wave pattern. Using 30 years of data, Namias showed that if the "tropospheric high pressure center in the Central Pacific is strong, there is a good probability of low heights along the West Coast and high heights over the Plains" (Namias, 1983). This further suggests that the cause for the stationary ridge is not completely local, and may have its origins in the Pacific.

Droughts in the western United States are also associated with an amplified tropospheric ridge, which is further west than for Great Plains droughts and in winter displaces storm tracks north of the United States/Canadian border. In winter, the ridge is also associated with an amplified Aleutian Low in the North Pacific, and this has been associated with forcing from the tropical eastern Pacific in conjunction with El Niño events (*e.g.*, Namias, 1978), whose teleconnection and resulting U.S. climate pattern has been discussed in Section 3.1.

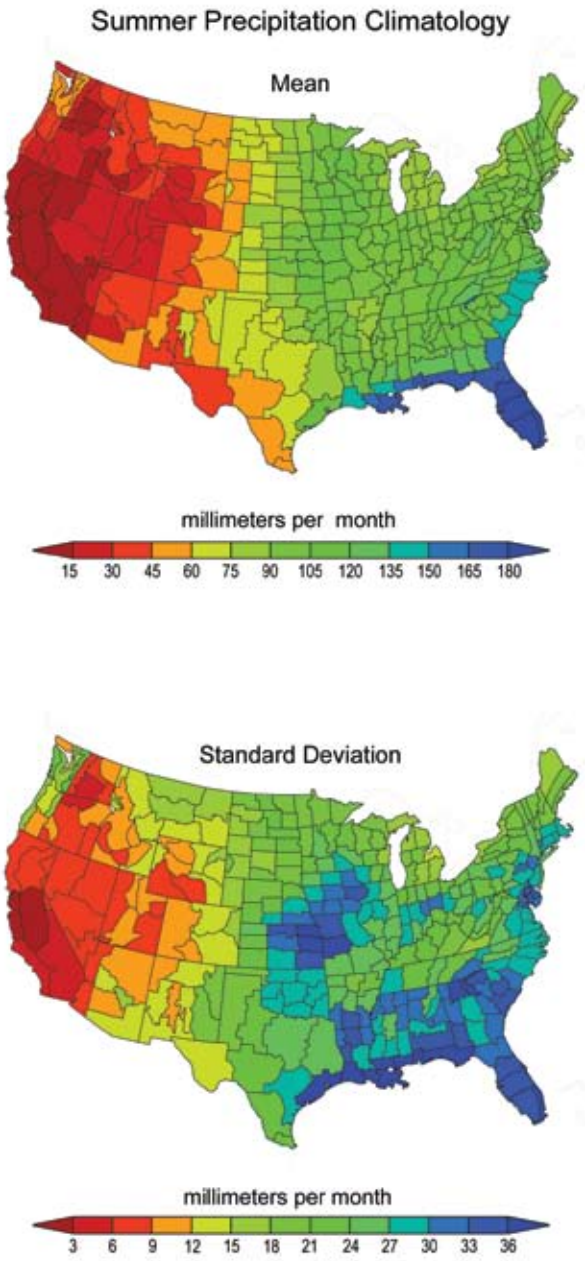

Figure 3.22 Climatological average (top) and standard deviation (bottom) of summer (June-July-August) seasonally-averaged precipitation over the continental United States for the period 1951 to 2006. Contour intervals are (a) 15 millimeters per month and (b) 3 millimeters per day (adopted from Ting and Wang, 1997). Data is the NOAA Climate Division dataset.

Could ENSO also be responsible for warm-season droughts? Trenberth *et al.* (1988) and Trenberth and Branstator (1992) suggested, on the basis of observations and a simplified linear model of atmospheric wave propagation, that colder sea surface temperatures in the tropical eastern Pacific (equatorward of 10°N), the La Niña phase of ENSO, in conjunction with the displacement of warmer water and the Intertropical Convergence Zone (ITCZ) northward

in that same region (15° to 20°N), led to the amplified ridging over the United States in the spring of 1988. While this was the leading theory at the time, the general opinion now is that most of the short-term summer droughts are more a product of initial atmospheric conditions (Namias, 1991; Lyon and Dole, 1995; Liu *et al.*, 1998; Bates *et al.*, 2001; Hong and Kalnay, 2002) amplified by the soil moisture deficits that arise in response to lack of precipitation (Wolfson *et al.*, 1987; Atlas *et al.*, 1993; Hong and Kalnay, 2002).

Warm conditions in the Indian Ocean/ West Pacific region are capable of instigating drought in the United States year round but especially in spring.

For droughts that occur for longer periods of time, various possibilities have been empirically related to dry conditions over specific regions of the United States and Canada. Broadly speaking, they are associated with the eastern tropical Pacific (La Niñas in particular); the Indian Ocean/West Pacific; the North Pacific; and (for the eastern United States) the western Atlantic Ocean. Cool conditions in the eastern tropical Pacific have been related to annual U.S. droughts in various studies (Barlow *et al.*, 2001; Schubert *et al.*, 2004, Seager *et al.*, 2005), although they are more capable of influencing the U.S. climate in late winter when the average atmospheric state is more conducive to allowing an extratropical influence (Newman and Sardeshmukh, 1998; Lau *et al.*, 2006). Warm conditions in the Indian Ocean/West Pacific region are capable of instigating drought in the United States year round (Lau *et al.*, 2006) but especially in spring (Chen and Newman, 1998). Warmer conditions in the North Pacific have been correlated with drought in the Great Plains (Ting and Wang, 1997) and the U.S. Northeast (Barlow *et al.*, 2001), although modeling studies often fail to show a causal influence (Wolfson *et al.*, 1987; Trenberth and Branstator, 1992; Atlas *et al.*, 1993). The North Pacific SST changes appear to be the result of atmospheric forcing, rather than the reverse; therefore, if they are contributing to drought conditions, they may not be the cause of the initial circulation anomalies. Alexander *et al.* (2002) concluded from Global Circulation Model (GCM) experiments that roughly one-quarter to one-half of the change in the dominant pattern of low frequency variability in the North Pacific sea surface temperatures during winter was itself the result of ENSO, which helps intensify the Aleutian Low and increases surface heat fluxes (promoting cooling).

Sea surface temperature perturbations downstream of North America, in the North Atlantic, have occasionally been suggested as influencing some aspects of U.S. drought. For example, Namias (1983) noted that the wintertime drought in the western United States in 1977, one of the most extensive far western droughts in recent history, appeared to be responsive to a downstream deep trough over the eastern United States. Warmer sea surface temperatures in the western North Atlantic have the potential to intensify storms in that region. Conversely, colder sea surface temperatures in summer can help intensify the ridge (*i.e.*, the "Bermuda High") that exists in that region. Namias (1966) suggested that such a cold water regime played an integral part in the U.S. Northeast spring and summer drought of 1962 to 1965, and Schubert *et al.* (2004) find Atlantic SST effects on the Dust Bowl, while multi-decadal swings between wet and dry periods over the United States as a whole have been statistically linked with Atlantic SST variations of similar timescale (McCabe *et al.*, 2004; Figure 3.5).

In Mexico, severe droughts during the reanalysis period were noted primarily in the 1950s, and again in the 1990s. The 1990s time period featured seven consecutive years of drought (1994 to 2000). Similar to the United States, droughts in Mexico have been linked to tropospheric ridges that can affect northern Mexico, and also to ENSO. However, there are additional

factors tied to Mexico's complex terrain and its strong seasonal monsoon rains. Mexican rainfall in the warm season is associated with the North American Monsoon System (NAMS), which is driven by solar heating from mid-May into July. Deficient warm season rainfall over much of the country is typically associated with El Niño events. La Niña conditions often produce increased rainfall in southern and northeastern Mexico, but have been associated with drought in northwestern Mexico (Higgins *et al.*, 1999). During winter and early spring, there is a clear association with the ENSO cycle (*e.g.*, Stahle *et al.*, 1998), with enhanced precipitation during El Niño events associated with a strengthened subtropical jet that steers storms to lower latitudes and reduced rainfall with La Niñas when the jet moves poleward.

Therefore, the occurrence of drought in Mexico is heavily dependent on the state of the ENSO cycle, or its teleconnection to the extratropics, and on solar heating variations. In the warm season there is often an out-of-phase relationship between southern and northern Mexico, and between spring and summer, dependent on the phasing of the NAMS (Therrell *et al.*, 2002). These aspects make attribution of recent droughts difficult. For example, the consecutive drought years from 1994 to 2000 occurred over several different phases of ENSO, suggesting multiple causes including El Niño conditions for warm season drought through 1998, the possible influence of Indian Ocean/West Pacific warming during the subsequent La Niña phase, and internal atmospheric variability.

Because a large proportion of the variance of drought conditions over North America is unrelated to sea surface temperature perturbations, it is conceivable that when a severe drought occurs it is because numerous mechanisms are acting in tandem. This was the conclusion reached in association with the recent U.S. drought (1999 to 2005) that affected large areas of the southern, western and central United States. During this time, warm conditions prevailed over the Indian Ocean/West Pacific region along with La Niña conditions in the eastern tropical Pacific—influences from both regions working together may have helped intensify and/or prolong the annual droughts (Hoerling and Kumar, 2003; Lau *et al.*, 2006).

3.5.3.2 Human influences on North American drought since 1951

To the extent that ENSO cycle variations (La Niñas in particular) are the cause of drought in the United States, it is difficult to show that they are related to greenhouse gas forcing. While some studies (*e.g.*, Clement *et al.*, 1996) have suggested that La Niña conditions will be favored as climate warms, in fact more intense El Niño events have occurred since the late 1970s, perhaps due at least in part to anthropogenic warming of the eastern equatorial Pacific (Mendelssohn *et al.*, 2005). There is a tendency in model projections for the future greenhouse-gas warmed climate to indicate an average shift towards more El Niño-like conditions in the tropical eastern Pacific Ocean, including the overlying atmospheric circulation; this latter aspect may already be occurring (Vecchi and Soden, 2007). With respect to the human influence on ENSO variability, Merryfield (2006) surveyed 15 coupled atmosphere-ocean models and found that for future projections, almost half exhibited no change, five showed reduced variability, and three increased variability. Hence, to the extent that La Niña conditions are associated with drought in the United States, there is no indication that they have been or will obviously be influenced by anthropogenic forcing.

Because a large proportion of the variance of drought conditions over North America is unrelated to sea surface temperature perturbations, it is conceivable that when a severe drought occurs it is because numerous mechanisms are acting in tandem.

However, given that SST changes in the Indian Ocean/West Pacific are a factor for long-term U.S. drought, a somewhat different story emerges. Shown in Figure 3.23 are the SST anomalies in this region, as well as the tropical central-eastern Pacific (Lau *et al.*, 2006). As noted with respect to the recent droughts, the Indian Ocean/West Pacific region has been consistently warm when compared with the 1971 to 2000 sea surface temperature climatology. What has caused this recent warming?

The effect of more frequent El Niños alone results in increased temperatures in the Indian Ocean, acting through an atmospheric bridge that alters the wind and perhaps the cloud field in the Indian Ocean region (Klein *et al.*, 1999; Yu and Rienecker, 1999; Alexander *et al.*, 2002; Lau and Nath, 2003); an oceanic bridge between the Pacific and the Indian Ocean has also been modeled (Bracco *et al.*, 2007). This effect could then influence droughts over the

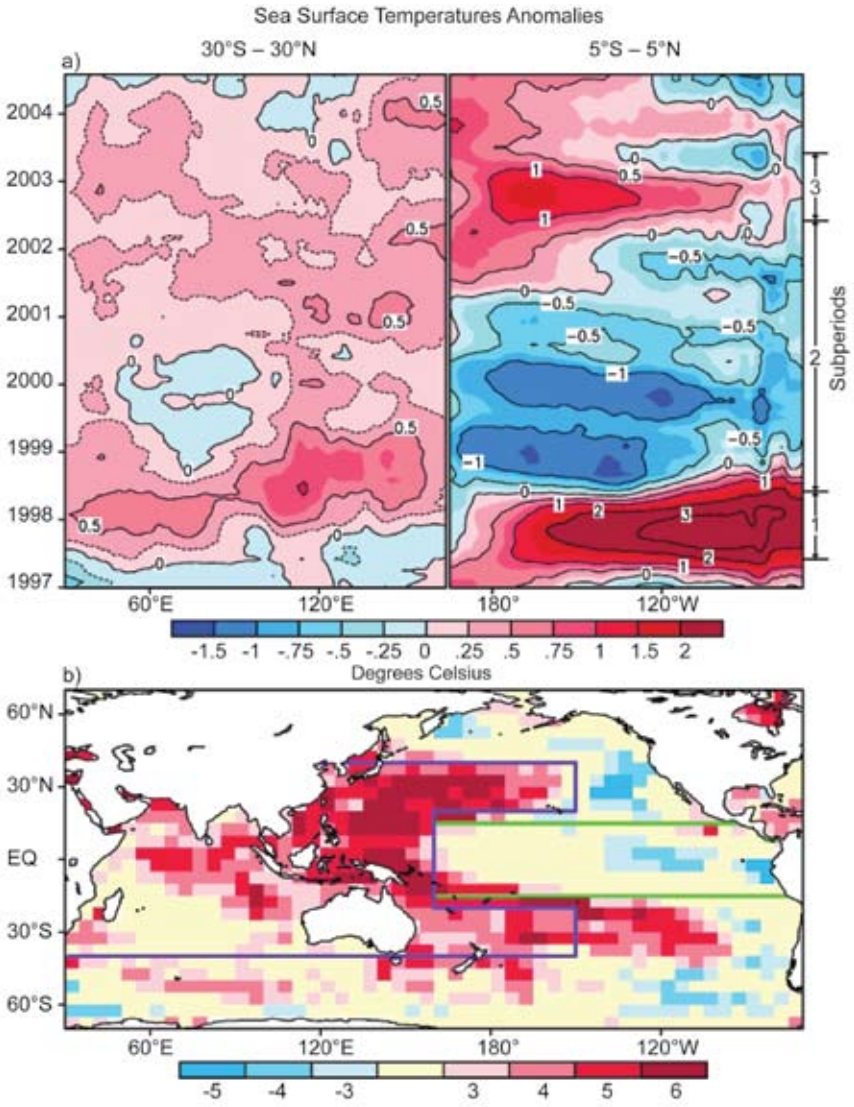

Figure 3.23 Top panel: Sea surface temperature anomalies relative to the period 1970 through 2000 as a function of year in the Indian Ocean/West Pacific (left) and central-eastern Pacific (right) (from Lau *et al.*, 2006). Bottom panel: Number of 12-month periods in June 1997 to May 2003 with SST anomalies at individual 5° latitude by 5° longitude rectangles being above normal (red shading) or below normal (blue shading) by more than one-half of a standard deviation (*i.e.* one-half the strength of the expected variability).

United States in the summer after an El Niño, as opposed to the direct influence of La Niña (Lau *et al.*, 2005).

Nevertheless, as shown in Figure 3.23, the warming in the Indian Ocean/West Pacific region has occurred over different phases of the ENSO cycle, making it less likely that the overall effect is associated with it. Hoerling and Kumar (2003) note that "the warmth of the tropical Indian Ocean and the western Pacific Ocean was unsurpassed during the twentieth century"; the region has warmed about 1°C (1.8°F) since 1950. That is within the range of warming projected by models due to anthropogenic forcing for this region and is outside the range expected from natural variability, as judged by coupled atmosphere-ocean model output of the CMIP simulations (Hegerl *et al.*, 2007). The comparison of the observed warm pool SST time series with those of the CMIP simulations in Section 3.2.2 indicates that it is very likely that the recent warming of SSTs over the Indian Ocean/West Pacific region is of human origins.

The possible poleward expansion of the subtropical region of descent of the Hadley Circulation is an outcome that is favored by models in response to a warming climate (IPCC, 2007a). It would transfer the dry conditions of northern Mexico to the U.S. Southwest and southern Great Plains; Seager *et al.* (2007) suggest that may already be happening, and is associated with drought in the southwestern United States. Additional observations and modeling improvements will be required to assess the likelihood of its occurrence with greater confidence.

An additional impact of greenhouse warming is a likely increase in evapotranspiration during drought episodes because of warmer land surface temperatures. It was noted in the discussion of potential causes that reduced soil moisture from precipitation deficits helped sustain and amplify drought conditions, as the surface radiation imbalance increased with less cloud cover, and sensible heat fluxes increased in lieu of latent heat fluxes. This effect would not have initiated drought conditions but would be an additional factor, one that is likely to grow as climate warms. For example, drier conditions have been noted in the northeast United States despite increased annual precipitation, due to a century-long warming (Groisman *et al.*, 2004); this appears to be true for Alaska and southern and western Canada as well (Dai *et al.*, 2004). Droughts in the western United States also appear to have been influenced by increasing temperature (Andreadis and Lettenmaier, 2006; Easterling *et al.*, 2007). The areal extent of forest fires in Canada has been high since

1980 compared with the previous 30 years and Alaska experienced record forest fire years in 2004 and 2005 (Soja *et al.*, 2007). Hence, by adding additional water stress global warming can exacerbate naturally occurring droughts, in addition to influencing the meteorological conditions responsible for drought.

A further suggestion of the increasing role played by warm surface temperatures on drought is given in Figure 3.24. A diagnosis of conditions during the recent U.S. Southwest drought is shown, with contours depicting the atmospheric circulation pattern based on reanalysis data, and shading illustrating the surface temperature anomaly (top) and precipitation anomaly (bottom). High pressure conditions prevailed across the entire continent during the period, acting to redirect storms far away from the region. Continental-scale warmth during 1999 to 2004 was also consistent with the anthropogenic signal. It is plausible that the regional maximum in warmth seen over the Southwest during this period was in part a feedback from the persistently below normal precipitation, together with the anthropogenic signal. Overall, the warmth associated with this recent drought has been greater than the warmth observed during the 1950s drought in the Southwest (Figure 3.21), likely augmenting its negative impacts on water resource and ecologic systems compared to the earlier drought.

Breshears *et al.* (2005) estimated the vegetation die-off extent across southwestern North America during the recent drought. The combination of drought with pine bark beetle infestation resulted in more than a 90 percent loss in Piñon pine trees in some areas. They noted that such a response was much more severe than during the 1950s drought, arguing that the recent drought's greater warmth was the material factor explaining this difference.

Current understanding is far from complete concerning the origin of individual droughts. While the assessment discussed here has emphasized the apparently random nature of short-term droughts, a product of initial conditions which then sometimes develop rapidly into strong tropospheric ridges, the relationships of such phenomena to sea surface temperature patterns, including the ENSO cycle, are still being debated. The ability of North Atlantic sea surface temperatures to influence the upstream circulation still needs further examination in certain circumstances, especially with respect to droughts in the eastern United States. The exact mechanisms for influencing Rossby wave development downstream, including the role of transient waves relative to stationary wave patterns, will undoubtedly be the subject of continued research. The Hadley Cell response to climate change, as noted above, is still uncertain. Also, while some modeling studies have emphasized the role played by surface

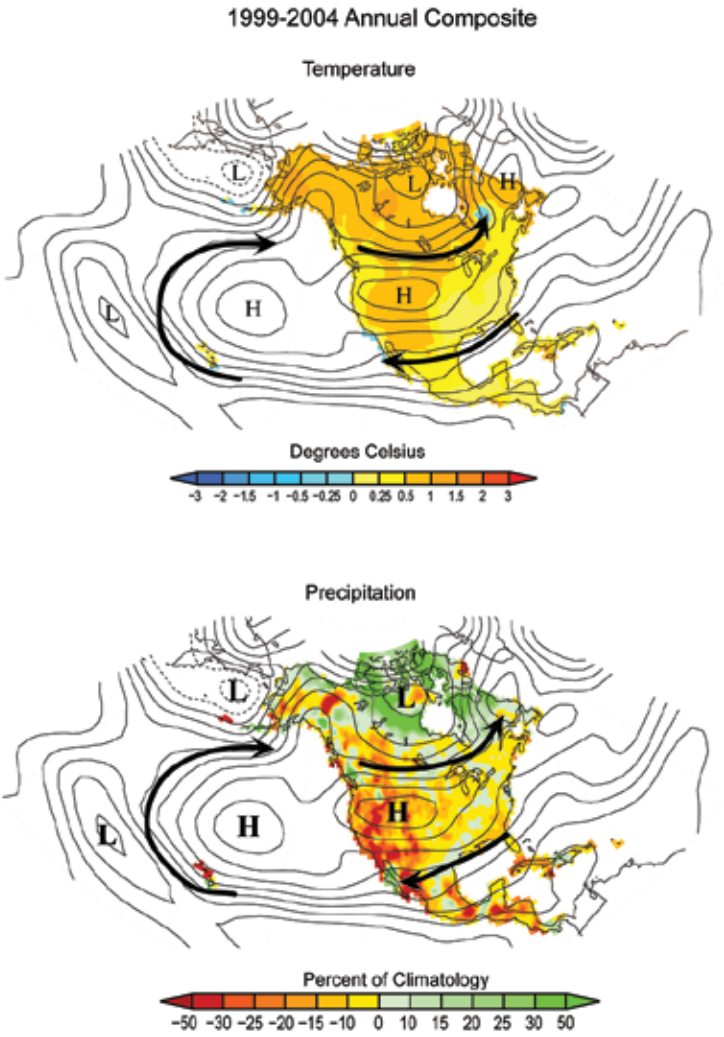

Figure 3.24 Observed climate conditions averaged for 1999 to 2004 during a period of severe southwestern U.S. drought. The 500 millibar height field (contours, units meters) is from the NCEP/NCAR R1 reanalysis. The shading indicates the five-year average anomaly of the surface temperature (top) and precipitation (bottom). The surface temperature and precipitation are from independent observational datasets. Anomalous High and Low Pressure regions are highlighted. Arrows indicate the anomalous wind direction, which circulates around the High (Low) Pressure centers in a clockwise (counterclockwise) direction.

The severity of both short- and long-term droughts has likely been amplified by local greenhouse gas warming in recent decades.

soil moisture deficits in exacerbating these droughts, the magnitude of the effect is somewhat model-dependent, and future generations of land-vegetation models may act somewhat differently.

Given these uncertainties, it is concluded from the above analysis that, of the severe droughts that have impacted North America over the past five decades, the short-term (monthly-to-seasonal) events are most likely to be primarily the result of initial atmospheric conditions, subsequently amplified by local soil moisture conditions, and in some cases initiated by teleconnection patterns driven in part by SST anomalies. For the longer-term events, the effect of steady forcing through sea surface temperature anomalies becomes more important. Also, the accumulating greenhouse gases and global warming have increasingly been felt as a causative factor, primarily through their influence on Indian Ocean/West Pacific temperatures, conditions to which North American climate is sensitive. The severity of both short- and long-term droughts has likely been amplified by local greenhouse gas warming in recent decades.